IMPACT OF HIGH PENETRATION OF SOLAR PVS ON HARMONICS IN LV DISTRIBUTION NETWORKS

R. O. Anurangi

158011U

Degree of Master of Science

Department of Electrical Engineering

University of Moratuwa
Sri Lanka

August 2018

IMPACT OF HIGH PENETRATION OF SOLAR PVS ON HARMONICS IN LV DISTRIBUTION NETWORKS

Rambukkanage Omesha Anurangi

158011U

Thesis submitted in partial fulfillment of the requirements for the degree of Master of Science in Electrical Engineering

Department of Electrical Engineering

University of Moratuwa

Sri Lanka

August 2018

DECLARATION

I declare that this is my own work and this thesis does not incorporate without acknowledgement any material previously submitted for a Degree or Diploma in any other University or institute of higher learning and to the best of my knowledge and belief it does not contain any material previously published or written by another person except where the acknowledgement is made in the text.

Also, I hereby grant to University of Moratuwa the non-exclusive right to reproduce and distribute my thesis, in whole or in part in print, electronic or other medium. I retain the right to use this content in whole or part in future works (such as articles and books).

……. Date:

R. Omesha Anurangi

The above candidate has carried out research for the Masters Dissertation under our supervision

1. Name of the supervisor:

…….. Date:

Dr. W. D. A. S. Rodrigo

2. Name of the supervisor:

……... Date:

Dr. (Mrs) U. Jayatunga

ABSTRACT

Present trend of using solar photovoltaic (PV) technology for generating electricity has marked a rapid growth in the number of grid connected solar PV systems which has been reported to make a considerable impact on the power quality in the grid. With comparison of power quality (PQ) problems such as voltage unbalance, local voltage rise and voltage fluctuations, the increase of network harmonic levels has been identified as a potential PQ concern with the grid connected solar PVs. PV inverters are source of harmonics that produces low order and high order harmonics at the switching frequency and its side bands. Low order harmonics present at the inverter output due to the inability of producing pure sinusoidal waveform. Varying solar irradiance, inverter characteristics, inverter capacity, multi-inverter interactions and background harmonic level are examples of factors which influence the amount of harmonic generation of a PV system.

This research focuses on the effect of high levels of harmonic injection and propagation of current harmonics in distribution network with solar PV integrations. A methodology is discussed in this thesis to achieve the aforementioned matter with the detailed modeling of PV inverters in a typical distribution network using PSCAD/EMTDC simulation platform. From the analysis of simulation results, the current harmonics injected by single phase inverters has been found substantial and influential with regard to the energy transmission and increase losses with compared to the three phase inverters. Unbalance occurred due to single phase inverters results in triplen harmonics to propagate to the upstream grid via the distribution transformer. Moreover, current harmonics superimposition were recorded as a result of multi-inverter operation. It was found that the Point of connection (POC) of the PV inverter affects the voltage harmonic levels at the inverter output.

Keywords - Harmonics; Photovoltaic inverters; Distribution Network; THD; Power Quality

ACKNOWLEDGEMENT

My sincere gratitude must go out to my supervisor Dr. Asanka S. Rodrigo, senior lecturer of the department of Electrical Engineering, University of Moratuwa. This achievement would not have been possible without the courage, guidance and assistance given to me throughout my research work.

My heartiest gratitude goes to my supervisor, Dr. (Mrs) Upuli Jayatunga, senior lecturer of the department of Electrical Engineering, University of Moratuwa in giving guidance, assistance and necessary resources focusing on the subject area.

Further, I would like to convey my grateful thank to Prof. J. P. Karunadasa for the assistance and encouragement given in this research which aided immensely in completing the study.

A special note of thank goes to my colleagues for their valuable assistance and support given to me which strengthened my work massively.

Finally, my unfeigned appreciation should go to my family, my beloved husband for his encouragement and support provided.

TABLE OF CONTENTS

LIST OF FIGURES

LIST OF TABLES

LIST OF ABBREVATIONS

NRE	non-renewable energy
RE	renewable energy
RER	renewable energy resource
CDM	clean development mechanism
ECF	energy conservation fund
NCRE	non-conventional energy resources
PV	photovoltaic
PQ	power quality
DC	direct current
AC	alternating current
THD	total harmonic distortion
IHD	individual harmonic distortion
THD%	percentage value of THD
SPWM	sinusoidal pulse width modulation
POC	point of connection
CSI	current source inverter
LV	low voltage
MPP	maximum power point
MPPT	maximum power point tracking
STC	standard test condition
InC	incremental conductance
PI	proportional-integral
IGBT	insulated gate bipolar transistor
ESR	effective series resistance
ESL	effective series inductance
MOSFET	metal oxide semiconductor field effect transistor
GTO	gate turn off

BJT	bipolar junction transistor
rms	root-mean-square
CEB	Ceylon Electricity Board
IPP	independent power producer
SPP	small power producer
LECO	Lanka Electricity Company (Private) Limited
OH	overhead
UG	underground
PSS	primary sub station
FDS	fuse disconnect switch
T-OFF	tap off
ABC	Aerial Bundled Cable
ADMD	after diversity maximum demand

LIST OF SYMBOLS

V_{THD}	THD of voltage signal
I_{THD}	THD of current signal
V_{THD}%	percentage value of V_{THD}
I_{THD}%	percentage value of I_{THD}
Ipv	output current of the PV array
Vpv	output voltage of the PV array
Vmppt	voltage at MPP
Vin	input voltage
Vout	output voltage
Iload	load current
fsw	switching frequency
L	inductance
R	resistance
C	capacitance
Cin	input capacitance
Cout	output capacitance
L_1	inductance of the inverter side inductor of the LCL filter
R_1	resistance of the inverter side inductor of the LCL filter
L_2	inductance of the grid side inductor of the LCL filter
R_2	resistance of the grid side inductor of the LCL filter
C_f	capacitance of the capacitor of the LCL filter
R_f	damping resistance of the LCL filter
E_n	inverter output rms voltage
P_n	rated active power
V_{dc}	dc voltage
f_g	fundamental frequency
Z_b	base impedance

C_b	base capacitance
ΔI_{Lmax}	maximum current ripple at the inverter output
N	number of customers
Dn	demand of customer n at the time of system maximum demand
P	active power
Q	reactive power
V	magnitude of the bus voltage
P_0	initial active power
Q_0	initial reactive power
V_0	initial value of V
Sout	output apparent power of the inverter
Iout	input current signal of the current source
Ppv	output real power of the PV array
Qpv	output reactive power of the PV array
T1	three phase inverter 1
T2	three phase inverter 2
T3	three phase inverter 3
S1	single phase inverter 1
S2	single phase inverter 2
S3	single phase inverter 3
F2-2	feeder 2 branch 2
F2-1	feeder 2 branch 1
V_{ab}	voltage between node a and b
V_{ao}	voltage between node a and o
V_{bo}	voltage between node b and o
V_{An}	voltage between node A and n
V_{Bn}	voltage between node B and n
V_{Cn}	voltage between node C and n
V_{Ao}	voltage between node A and o

V_{Bo}	voltage between node B and o
V_{Co}	voltage between node C and o
h	harmonic order
t_0	starting time
T	periodic time
I_{An}	output current of the inverter
Z_S	source impedance
Z_T	transformer impedance
Z_G	resultant grid impedance
Z_h	impedance at h^{th} harmonic frequency
V_h	harmonic voltage at h^{th} harmonic frequency
I_h	harmonic current at h^{th} harmonic frequency

Chapter 1

1. INTRODUCTION

1.1. Background

Energy resources can be categorized into two groups; non-renewable energy (NRE) and renewable energy (RE). Fossil fuels like coal, petroleum and natural gas are examples of NRE resources which can be extracted naturally to generate electricity. But, these are naturally replenished slower than these are being utilized. In addition, nuclear fission is also considered as a NRE resource and an alternative energy option. The adverse effect of NRE such as carbon output, unhealthy gas emissions; carbon dioxide which causes global warming and Sulphur dioxide which creates acid rain and environmental pollution can be marked.

Renewable Energy Resources (RER) are those sources of energy are not depleted as these are consumed. RERs include wind, solar geothermal, hydro power, tidal, ocean wave, ocean thermal and biomass. At present, RERs become more common, popular for electricity generation because of the cleanliness, in abundant supply and zero greenhouse gas emission to serve the increasing power demand effectively. Some of RERs such as wind, solar, bio-mass and small-scale hydro power are good resources of providing electricity at distributed levels [1][2]. They are the leading non-conventional forms of renewable energy promoted in Sri Lanka for electricity generation in to the grid. The government will endeavor to reach a minimum level of 10% of electrical energy supplied to the grid to be from NRE, facilitating Clean Development Mechanism (CDM) from the year 2015 onwards. The government may subsidize the energy utilities for this process to achieve it without causing additional burden on the end user tariffs. The "Energy Fund "which is managed by the Energy Conservation Fund (ECF) will provide incentives for the promotion of Non-Conventional Energy Resources (NCRE) and strengthen the transmission network to absorb the NCRE technologies in to the grid [3].

It is clear that the vision of the power and energy sector of Sri Lanka is to capture the full potential of all renewable resources to be an energy self-sufficient nation, lowering the expenditures for importing fossil fuels, crude oil, refined petroleum products and coal annually [4].

With comparison to other forms of RE sources, the use of solar power is more popular due to its advantages such as faster implementation, economically viable investment and especially the freely availability of solar energy. The abundant solar radiation which ranges from 4.5 to 6.0 kWh/m^2 and recent national level policies such as net metering, net accounting are driving factors to develop solar photovoltaic (PV) technology among both the public and private sectors in Sri Lanka. The project titled "Battle for Solar Energy" expects to install 200 MW of solar electricity by 2020 and 1000 MW by 2025 [5]. Currently, the installed capacity of solar PV has reached the level of 100 MW as shown in Figure 1.1.

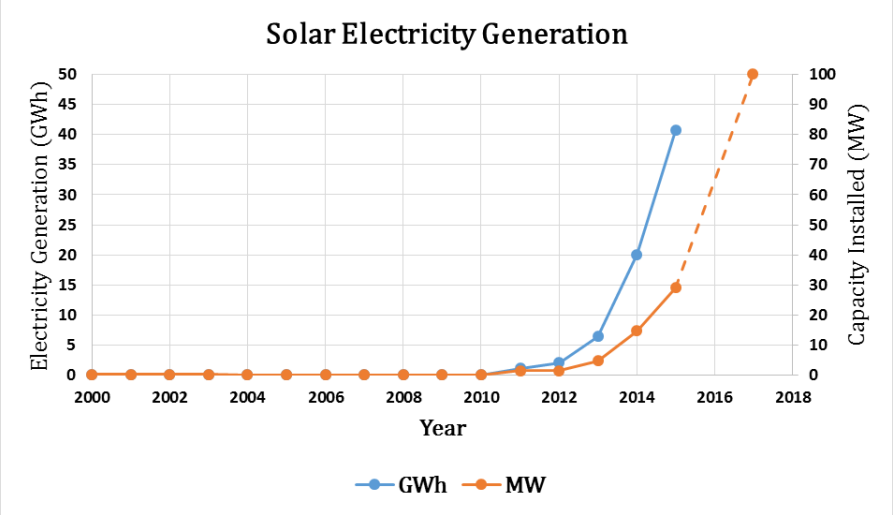

Figure 1.1: Solar PV installed capacity in Sri Lanka from 2000-2015 [5]

Although the solar PV technology is advantageous, a challenge exists with its intermittency and randomness, rendering it hard to match supply and demand. Further, Solar PV integrations degrade the supply quality progressively in different aspects. The key issues imposed by solar PV pertaining to Power Quality (PQ) can be identified as an increased level of harmonics, voltage unbalance, deterioration of power factor and voltage regulation in the distribution networks. Among these PQ problems, the increase of network harmonic levels due to PV systems is most dominant as it is very much difficult to restrict. Power electronic techniques used in solar PV in DC to AC inversion cause the harmonic generation. Moreover, harmonic issue is worsen by the presence of non-linear loads at the vicinity of solar installations [6][7].

The Total Harmonic Distortion (THD) is the most common and simple indicator to evaluate the harmonic content of a particular signal; voltage or current. The Individual Harmonic Distortion (IHD) also measure the magnitude of individual harmonic components as a percentage of the fundamental component. There are number of standards such as IEEE standards 519-1995, Australian standards AS 4777.2, British standards EN61727 and IEC 61000-3-2:12. IEEE 1547-2003 and IEC 61727:2004 which provide technical details of current and voltage harmonic distortion levels and describe the interconnection requirements of the distributed generation units; PV inverters to the utility distribution network [8][9].

1.2. Problem Statement

A large number of solar PV integrations varied from medium to small scale, particularly residential roof-top PV system integrations will create many technical challenges to the power distribution utilities to conserve their traditional policies, regulations and to change them appropriately. Harmonic level in the distribution network due to this higher penetration of solar PV systems will be increased. Therefore, an exceptional study of PV penetration is required to minimize the adverse effects imposed by these PV inverter harmonics in the distribution network to maintain a healthy power system.

Electrical power generation of a solar PV system merely influenced by input quantities like solar irradiance and temperature. Fluctuations in these factors immediately affect the power output of the system accordingly the current output. Then it will result in changes in individual harmonic levels as well as the THD levels. Uneven distribution of single phase PV systems among three phases may lead an unbalance in the power system causing unacceptable voltage unbalances. Even though the PV systems are manufactured with harmonic mitigation techniques and satisfying harmonic standards, there are several factors that can influence the harmonic generation of these PV systems. The harmonic generation can be affected by the interactions of the grid connected harmonic sources like non-linear loads including adjacent PV inverters. Different manufactures follow different types of control strategies, different capacities and different filtering circuits. Therefore, the harmonic generation of these PV inverters will be divergent.

1.3. Objective and Methodology

The main objective of this research is to examine the harmonic penetration in distribution networks caused by increased PV integrations. This study incorporates the harmonic generation due to the different configurations of solar PV inverters, propagation of harmonics in distribution network and the effect on harmonics with the presence of multi-inverter interactions.

This objective is achieved through the following methodology.

- A typical PV system and a distribution network were modeled using PSCAD/EMTDC simulation platform. Both single phase and three phase inverters were designed in same format and same inverter control topology.
- Harmonic generation of single phase and three phase inverters was studied with different combinations of multiple inverter integrations by using detailed models of solar PV systems.
- Single phase and three phase inverter integrations were changed to examine the effect of POC s of PV systems on harmonics.
- Solar irradiance was reduced to study the impact on harmonic level at the single phase and three phase PV system outputs.
- To investigate the propagation of low order harmonics, a PV system was modeled as a current source and named as 'harmonic injector'.
- Conclusions were made with a proper analysis of simulation results.

.

1.4. Outline of the Thesis

This section presents a brief description of the content of the thesis. Chapter 2 gives a concise literature review of effect of harmonics in a distribution network with solar PV integrations. It concludes findings from simulation results and analyses using experimental, actual data. Chapter 3 explains the detailed modeling of a solar PV system with its typical components. Further, it describes the distribution network and load modeling of an existing distribution feeder with its actual data. Chapter 4 is the analysis of simulation results of the detailed model integrations. Moreover, it presents the performance of the grid connected solar PV system under different scenarios. In

chapter 5, modeling of a generalized unit to represent a PV system as a current source inverter (harmonic injector) is discussed. Further, the simulation results of this harmonic injector integrations and its analysis are given here. Chapter 6 is the discussion and conclusion of this research study. Discussion contains the routine of the development of PSCAD models of solar PV system, distribution network and the manner the objective is succeeded. Conclusion consists of important findings of this research study.

2. LITERATURE REVIEW

2.1. Harmonics

The presence of harmonics in an electrical system results in distortion of the sinusoidal waveform of current or voltage. They widely accepted method of analyzing harmonics is using Fourier series which represents a non-sinusoidal waveform as an infinite sum of sinusoidal waveforms that are an integral multiple of fundamental frequency [10][11]. These multiples are called "harmonics" of the fundamental signal.

The rms value of the signal f(t) can be expressed in terms of rms value of its harmonic as;

$$F = \sqrt{{F_0}^2 + + \sum_{h=1}^{\infty} {F_h}^2} \quad (2.1)$$

Where, F_0 – dc component of the signal

F_h – h^{th} harmonic component of the signal

Furthermore, the term inter-harmonics is well defined in IEC-1000-2-1. But, subharmonics do not have official definition [12].

Inter-harmonics are the signals which the frequency are not positive integer multiples of the fundamental frequency. Table 2.1 provides mathematical definitions of dc component, harmonics, inter-harmonics and sub-harmonics.

Table 2.1: Definitions of dc, harmonic, inter-harmonic and sub-harmonics [12]

Harmonic	$f = h \times f_1$ where h is an integer > 0
DC	f = 0 Hz ($f = h \times f_1$ where h = 0)
Inter-harmonic	$f \neq h \times f_1$ where h is an integer > 0
Sub-harmonic	f > 0 Hz and $f < f_1$
Where, f_1 = fundamental frequency h = harmonic order	

The amount of harmonic distortion of voltage or current is quantified as a percentage of the fundamental with the index called "Total Harmonic Distortion (THD)" [10]. The THD of a signal F is defined as;

$$F_{THD}\% = \sqrt{\sum_{h=2}^{\infty} \left(\frac{F_h}{F_1}\right)^2} \times 100 \quad (2.2)$$

The power system consists of simply series and shunt elements. Moreover, the magnetizing impedance of the transformer and loads are the shunt elements while the leakage impedance of the transformer and series impedance of the power delivery path are the series elements of the power system. It is convenient that the nonlinearity is caused by the shunt elements in which the current is not proportional to the applied voltage. These are the harmonic sources which inject harmonic currents in to the power system.

The voltage distortion occurs when the distorted current travelling through the linear, series impedance of the power delivery path. Figure 2.1 explains that at the time which a non-linear load draws a distorted current, as it passes through the series impedance then results in a voltage drop for each harmonic. Therefore, it causes a voltage harmonic distortion at the load. The amount of the distortion depends on the impedance and the current [13].

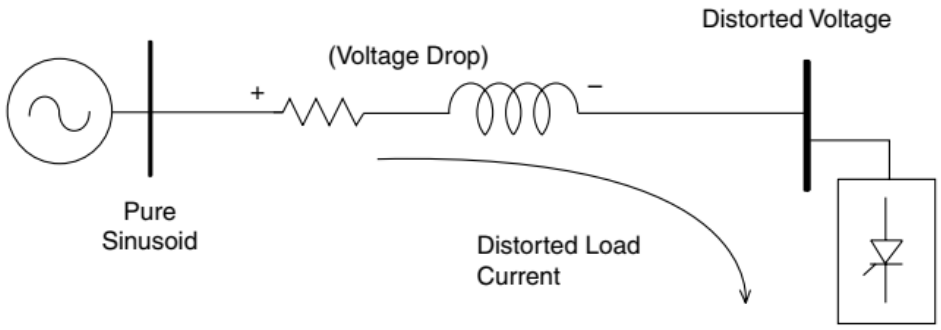

Figure 2.1: Harmonic currents flowing through the system impedance result in harmonic voltages at the load [13]

When the waveform possess the odd symmetry (i.e. positive and negative half cycles of the waveform have identical shapes) the Fourier series contains only odd harmonics. This will further simplify the study of harmonics in a power system [10].

2.2. Harmonics from Grid-Connected Solar PV

The harmonic emission from PV inverters which are in the market at present are different according to their characteristics such as size of the inverter, switching algorithm, power electronic circuit topologies. Harmonics produced by a PV system can be basically identified in two ways as primary emission and secondary emission.

Primary emission is caused by the inverter operation due to its power electronics. This is originating from the inverter. Then, this can be classified into two as low order harmonic and high order harmonics. Low order harmonics are originated as the switching technique cannot produce purely sinusoidal output. These are the harmonic components up to 40^{th} order (i.e. up to2 kHz for a 50 Hz system). High order harmonics are created by the switching of the power switches at the switching frequency and its side bands. These are greater than the harmonic order of 40 (i.e. greater than 2 kHz for a 50 Hz system). Primary emission does not depend on the power output of the inverter. The source impedance seen at the inverter output and the ambient voltage distortion at the inverter output affect the primary emission. But, interactions between inverter and the grid connected other devices can be observed which affect the primary emission too. Secondary emission is caused by the interactions between grid side filter circuit and the grid connected other devices. It depends on the background voltage distortion and the input impedance of the PV system. Harmonic content in secondary emission may have high order harmonics due to a connection of high order harmonic source nearby [14]. Figure 2.2 shows generalized model of a grid connected PV system which explains primary emission and secondary emission further.

The primary emission can be expressed as;

$$I_1 = \frac{Z_1}{Z_1+Z_2} J_1 \tag{2.3}$$

The secondary emission can be expressed as;

$$I_2 = \frac{1}{Z_1+Z_2} E_2 \tag{2.4}$$

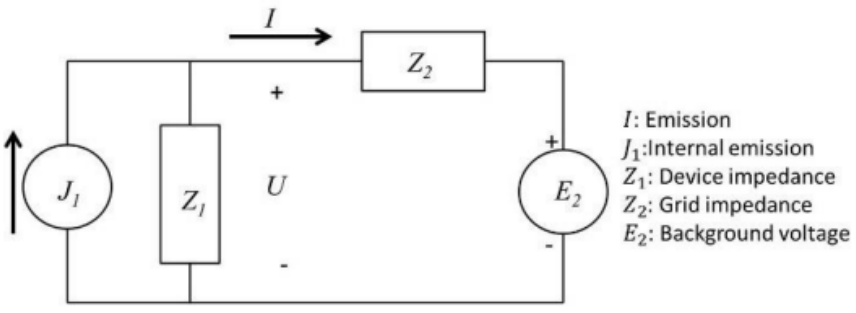

Figure 2.2: Simplified diagram of a grid connected PV system [14]

Generally, the past research findings related to grid-connected PV system harmonics can be categorized into four sections.

1. Harmonic generation
2. Effect of point of connection on harmonics
3. Effect of multi-inverter operation on harmonics
4. Effect of solar irradiance on harmonics

2.2.1. Harmonic generation

PV inverters produce harmonics, subharmonics and inter-harmonics depending on the inverter characteristics such as switching technique, switching frequency, inverter topology and network characteristics (i.e. Strong/Weak). In Sinusoidal Pulse Width Modulation (SPWM), harmonic generation can be controlled with the selection of switching frequency to achieve synchronous PWM. It describes more, the PV inverter output does not possess any subharmonics. Further, If the frequency modulation index (m_f), explained by Eqn. 2.5 is an odd integer, it will cancel the coefficients of cosine terms in Fourier series, resulting in only odd harmonics in the harmonic spectrum.

$$m_f = \frac{\text{Switching frequency } (f_{sw})}{\text{Grid frequency } (f_g)} \tag{2.5}$$

SPWM endorses less low-frequency harmonics in the harmonic spectrum of the inverter output if it satisfies the linear modulation. Moreover, if the amplitude modulation index (m_a) as given by Eqn. 2.6 is greater than one, which violates the linear modulation and is called over modulation then low frequency harmonics are appeared at the inverter output [15].

$$m_a = \frac{\text{peak amplitude of the fundamental frequency component}}{\text{amplitude of the carrier signal}} \tag{2.6}$$

Therefore, selecting a switching frequency and switching technique are influential factors which can be used to mitigate the harmonics at the PV system output. In following cases, authors had not considered that criteria in selecting the switching frequency for their applications. In some studies, the switching technique is not mentioned.

A. Y. kalbat states that simulation results of a three phase inverter harmonic spectrum at the inverter output, which is connected to a grid with galvanic isolation. Author uses SPWM, system frequency is 60 Hz and m_f is not an odd integer. Therefore, even harmonics are appeared at the harmonic spectrum as shown in Figure 2.3 [16].

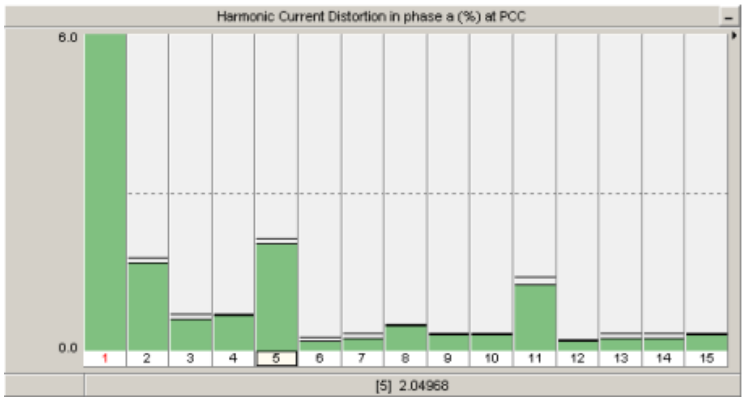

Figure 2.3: Harmonic current distortion in phase A (%) at PCC [16]

In the experiment of D. G. Infeild, harmonic measurements of a single phase inverter which is connected to a single phase supply with no intervening transformer prove that even harmonics are available in the spectrum where the m_f is an even integer. In this experiment, system frequency is 50 Hz and the switching frequency is 20 kHz [17]. Figure 2.4 provides the percentage magnitude of current harmonics.

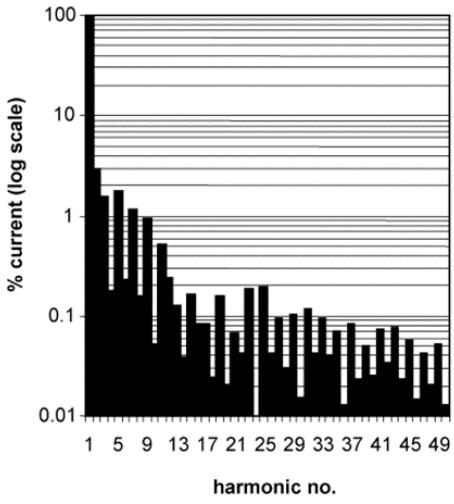

Figure 2.4: Percentage magnitude of current harmonics [17]

In most of the cases, the switching frequency was selected in the range of 10 – 20 kHz. Therefore, the harmonics produced by the PV system at the switching frequency and its bands are higher order harmonics which exceed the harmonic order of 200. When the THD s are calculated, these harmonics were not considered which can influence the THD value extremely [16-18].

The background distortion is an important factor which affect the harmonic generation of a solar PV system. Increasing of harmonic level in the distribution network will multiply the harmonic level at the PV inverter output. When a PV system is connected to a distorted voltage supply, harmonic production will be worsen and even inverter can be tripped. In [18], experimental results show that the influence of the background distortion. Three cases; case 1- with a sinusoidal supply, case 2 – with 3% of THD and case 3 – with 8% of THD. Figure 2.5 clearly shows that the distortion of inverter outputs.

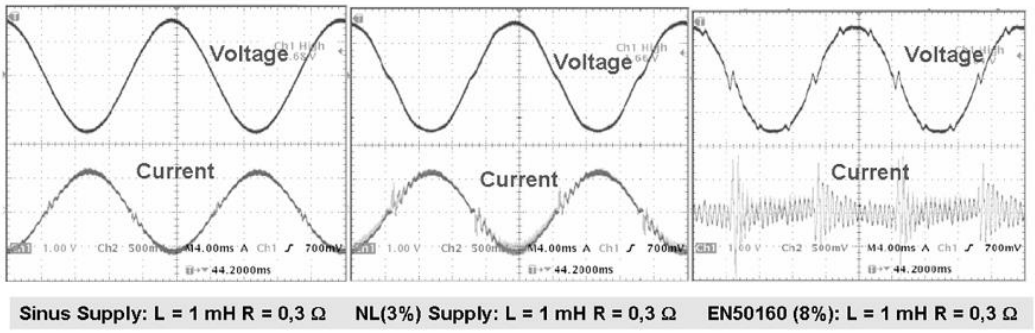

Figure 2.5: Distorted waveforms due to background harmonic level [18]

2.2.2. Effect of point of connection (POC) on harmonics

The voltage THD levels are increasing from upstream to downstream nodes while current THD levels are following an opposite trend; higher values at nodes which are close to the distribution transformer due to a decrease in current magnitudes with PV penetration. The voltage drop along the distribution feeder causes the increase in voltage THD [19]. Figure 2.6 proves that the trend of the voltage THD and the current THD along the distribution feeder. At the secondary of the transformer, it has given lower individual voltage harmonic values than the location 2145BhE which is far-end point in the feeder. Current harmonics levels of above two location has been marked as higher value at the transformer secondary than the location 2145BhE.

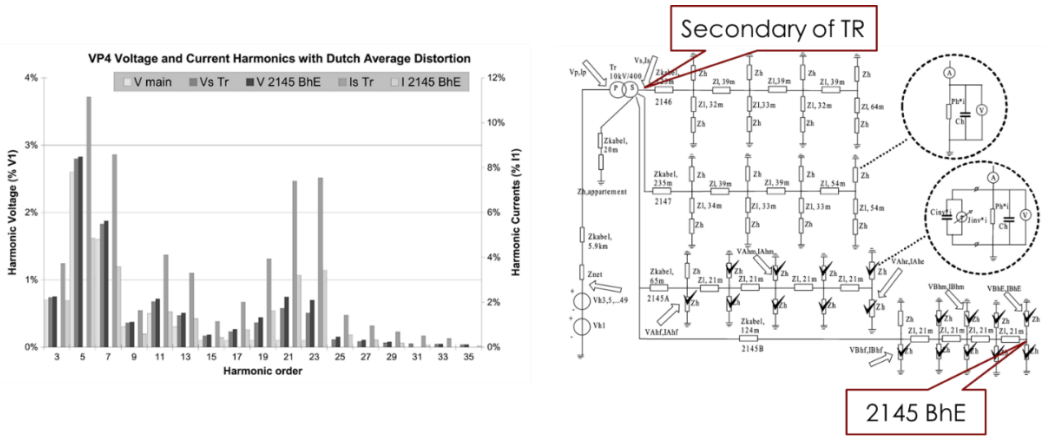

Figure 2.6: Harmonic spectrum measured at two different locations in the distribution network [18]

In [18], two locations in the distribution feeder are not sufficient to conclude the variation of THD of voltage and THD of current. Conveniently, more locations should be selected in the distribution feeder to connect solar PV systems and to measure harmonic levels by increasing the distance from distribution transformer to a particular location.

The simulation results in [20], state that there is an increase in THD of voltage noticeably when the POC of the inverter is close to the end of the feeder. Further, the values do not violate the limitations given by IEEE 519-1992 as the network has zero ambient harmonic distortion.

2.2.3. Effect of multiple inverter operation on harmonics

Cancellation and attenuation of individual harmonics are the consequences of multiple solar PV system integrations. Harmonic currents are influenced by the background voltage distortion. Additionally, Injection of harmonic currents causes voltage distortion which affect the other devices harmonic production. As a result of the particular phenomena, it attenuates the currents causing the disturbance. Cancellation occurs due to the aggregation of harmonic currents in the same frequency – out of phase. Harmonic currents of same frequency add up and the magnitude will depend on the phase difference [21]. It has been shown that, some inverter-inverter interactions

cause an increment in THD when the number of grid-connected inverters is increased [17][20]. Figure 2.7 proves the variation of THD with the number of inverters.

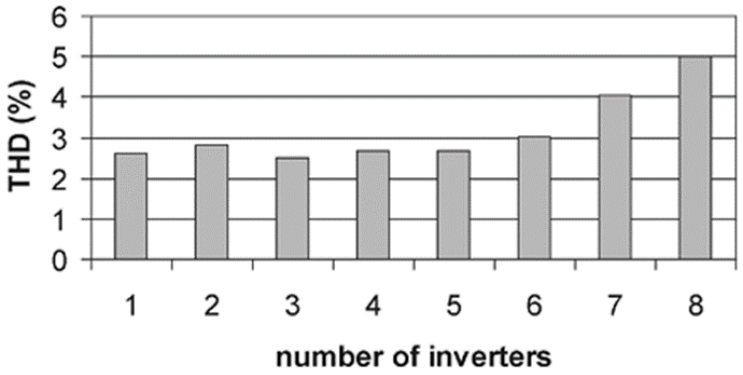

Figure 2.7: THD variation with the number of connected inverters [17]

Also, very limited attenuations are recorded due to the interaction between identical inverter integrations. Cancellations of low order harmonics are noticed if the phase angles are gathered about a value and equal in magnitude, resulting in a reduction in THD [22].In [22], by using data from an experimental system it was recorded that the voltage magnitude of individual harmonics is being increased when the number of grid connected inverters is increased as illustrated in Figure 2.8.

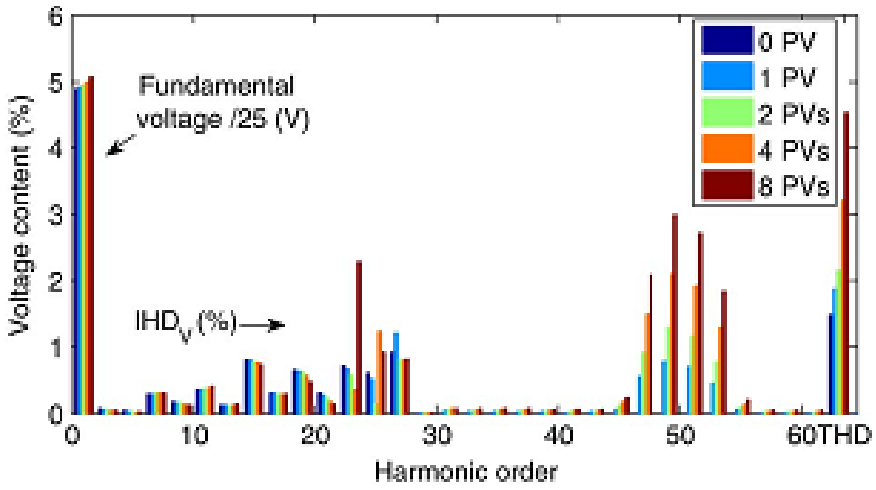

Figure 2.8: Individual harmonic percentage values with different number of PV integrations [22]

2.2.4. Effect of solar irradiance on harmonics

As given in Table 2.2, some experimental results from [23] show that current THD s

at partially cloudy days exceeds the standard limit of 5% and current THD s are less than 5% at sunny days.

Table 2.2: Experimental current THD values of five different PV inverters [23]

Average values of THD_I for clear sky days, $\overline{THD_I^c}$, and partially cloudy days, $\overline{THD_I^p}$

	Sunnuy Boy 2400	Tauro PRM3	Sun Profi 2400	Ingecon Sun 2500	Solete 2500
$\overline{THD_I^c}$	3.6	2.9	2.7	5.8	4.4
$\overline{THD_I^p}$	6.3	5.7	4.7	10.0	8.7

The current THD depends on the inverter output power. Solar irradiance which incident on the PV array decide the power output of the PV array. Hence, the variation of the inverter output power. If P_0 is the rated output power of the PV inverter the relationship between current THD and P_0 can be stated as given in Eqn. 2.7.

$$\text{current THD} = AP_0^{-B} \tag{2.7}$$

Where A and B are characteristic constant of each inverter.

A is the current THD when the inverter works at its nominal power. A and B can be estimated by using Eqn. 2.8,

$$\ln(\text{current THD}) = \ln A - B \ln P_0 \tag{2.8}$$

Test results of a single phase inverter are given in Figure 2.9, estimated values of A and B are given in the graph as well [23].

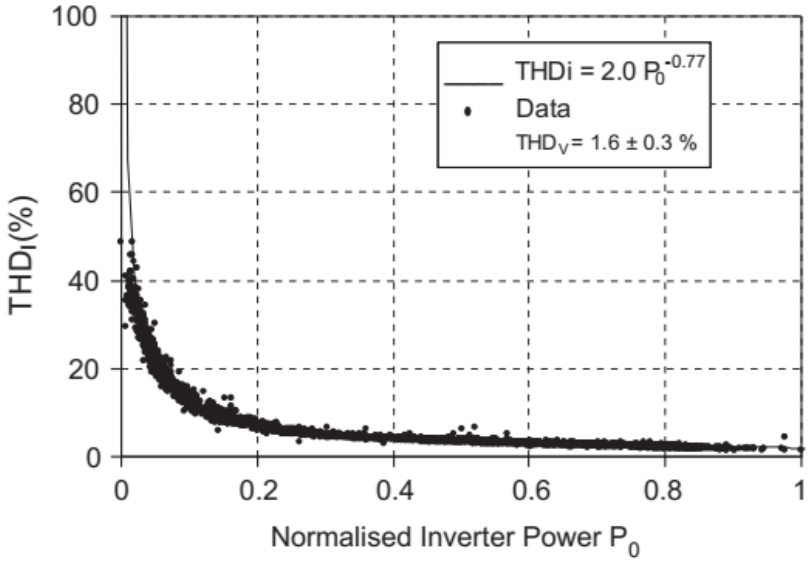

Figure 2.9: Current THD variation with the power output of the inverter [23]

In [24], observations obtained by analyzing measurements from a grid connected PV site prove that the effect of the variation of solar irradiance on both voltage and current THD s. It implies that the voltage THD does not possess a strong variation due to the change of solar irradiance. But, the current THD is dramatically affected by the low solar irradiance as it varies from 6% to 65% which was observed from the

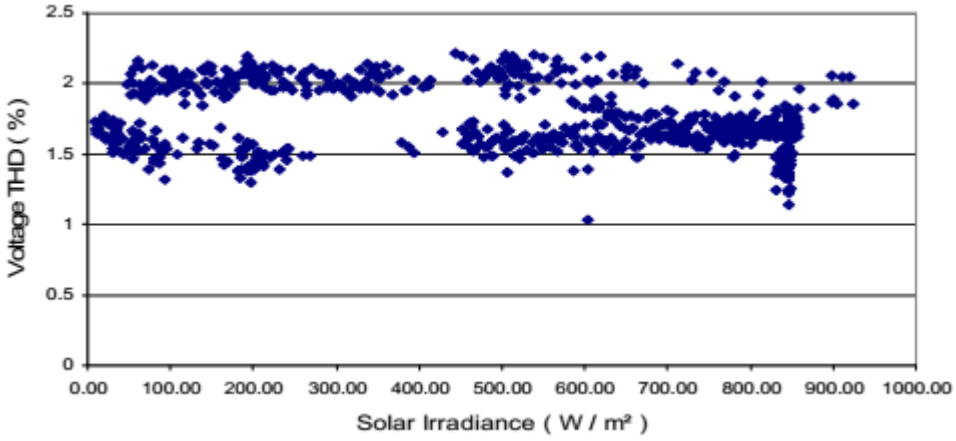

Figure 2.10: Variation of voltage THD with solar irradiance [24]

measurements of a grid connected PV site. The variation of Voltage THD and current THD against the solar irradiance are shown in Figure 2.10 and Figure 2.11 from [24].

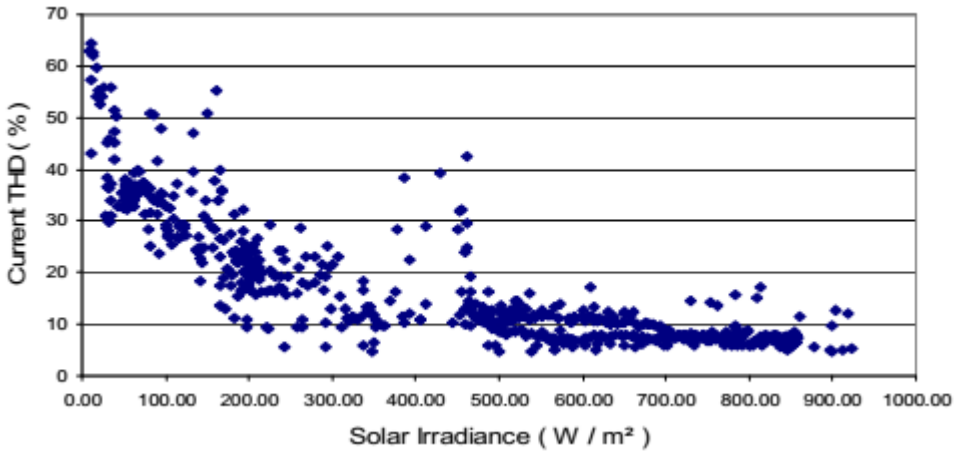

Figure 2.11: Variation of current THD with solar irradiance [24]

There are some evidence of increase in individual current harmonic distortions at low output power of the inverter. Obviously less solar irradiance will result in a low ac power output from the PV system. Further, the inverter is not capable of working at its

rated power due to this intermittency of solar irradiance. Then, these test results of individual harmonic current emissions of single phase and three phase inverters show that an increment in harmonic currents when the inverter works at low power [21].

Chapter 3

3. MODELING OF PV SYSTEMS AND THE NETWORK

In this research, the entire system containing single phase/three phase inverters and the utility grid were modeled in versatile and powerful PSCAD/EMTDC simulation platform which has been widely used by researchers in the power system field [25].

3.1. Detailed PV System Modeling

In order to investigate the behavior of solar inverters in relation to harmonic injections, a comprehensive solar PV model was developed accommodating different configurations.

A typical PV system consists of a PV array, DC-DC Converter with Maximum Power Point Tracking (MPPT) unit, Inverter Bridge, inverter controlling unit and the filter circuit as shown in Figure 3.1. Component assembling and modeling were succeeded according to the guidance described in [26][27].

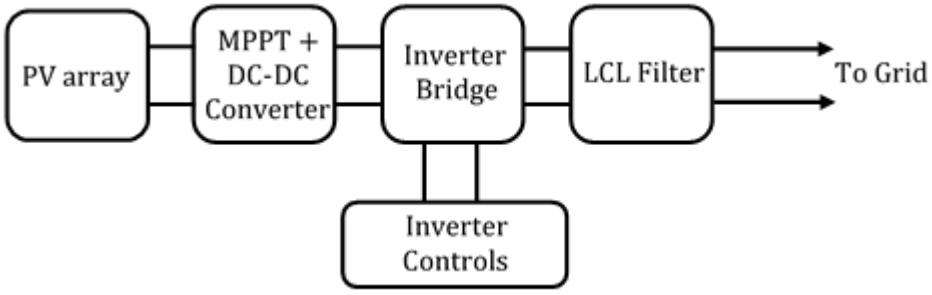

Figure 3.1: Components of a typical PV system

3.1.1. PV array

The PSCAD library model of PV array was used with its default values which are given in Table 3.1. Some changes were made in the numbers of cells connected in series/parallel per module and numbers of modules connected in series/parallel per array to achieve the required power rating of 2 kW and the DC voltage to feed the inverter bridge for single phase and three phase inverters separately.

Figure 3.2 (a) and 3.2 (b) are the characteristic curves (Power Vs Voltage) of PV arrays which were used in single phase and three phase inverter operation

respectively. The PV arrays were operated under Standard Test Conditions (STC); the solar irradiance intensity of 1000 W/m^2 and the cell temperature 25 ^{0}C [27].

Table 3.1: Default PV cell parameters

Effective area / cell	0.01 m^2
Series resistance	0.02 Ω
Shunt resistance	1000 Ω
Diode ideality factor	1.5
Band gap energy	1.103 eV
Saturation current at reference conditions / cell	1e^{-12} kA
Short circuit current at reference conditions / cell	0.0025 kA
Temperature coefficient of photo current	0.001 (A/K)

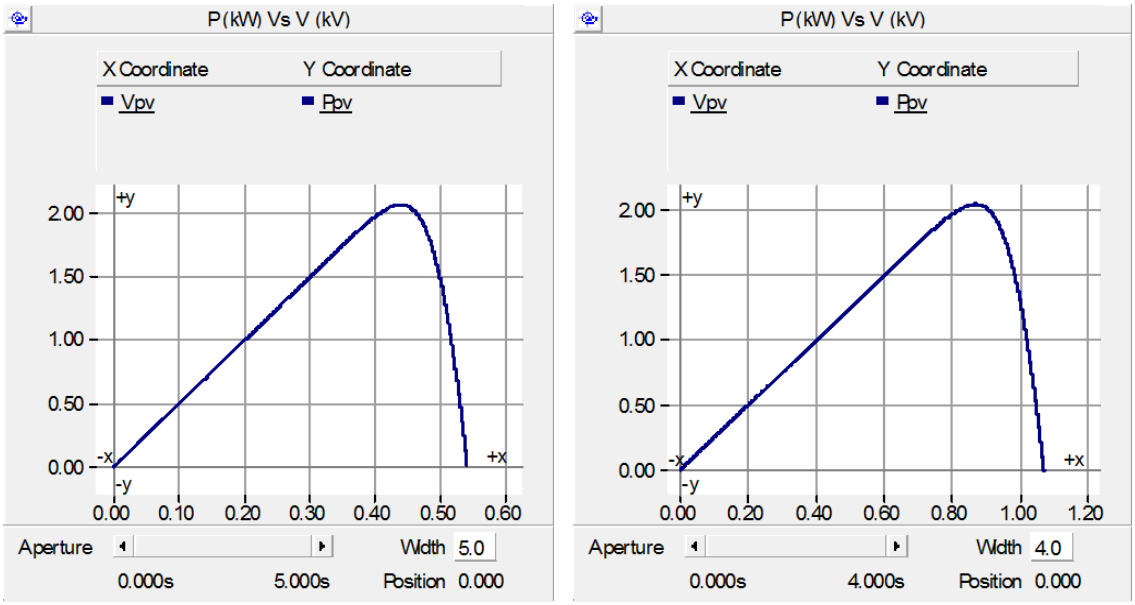

(a) (b)

Figure 3.2: Power Vs Voltage characteristic curves

3.1.2. Maximum power point tracking and DC-DC converter

The output current (Ipv) and the output voltage (Vpv) of the PV array were passed through a first order low pass filter with the default gain of 1 and the time constant 0.01 s [27] to avoid high frequency components from these two signals. Then filtered

Ipv and Vpv were fed in to the MPPT unit and the Incremental Conductance (InC) tracking algorithm was selected for MPP tracking. The error signal; the difference of the Vpv and MPP voltage (Vmppt) was sent through a Proportional Integral (PI) controller. Later, the output of the PI controller is compared with a saw tooth signal which varies between 0 and 1to produce the firing signal (T1) for the Insulated Gate Bipolar Transistor (IGBT) switch in the DC-DC converter as shown in Figure 3.3.

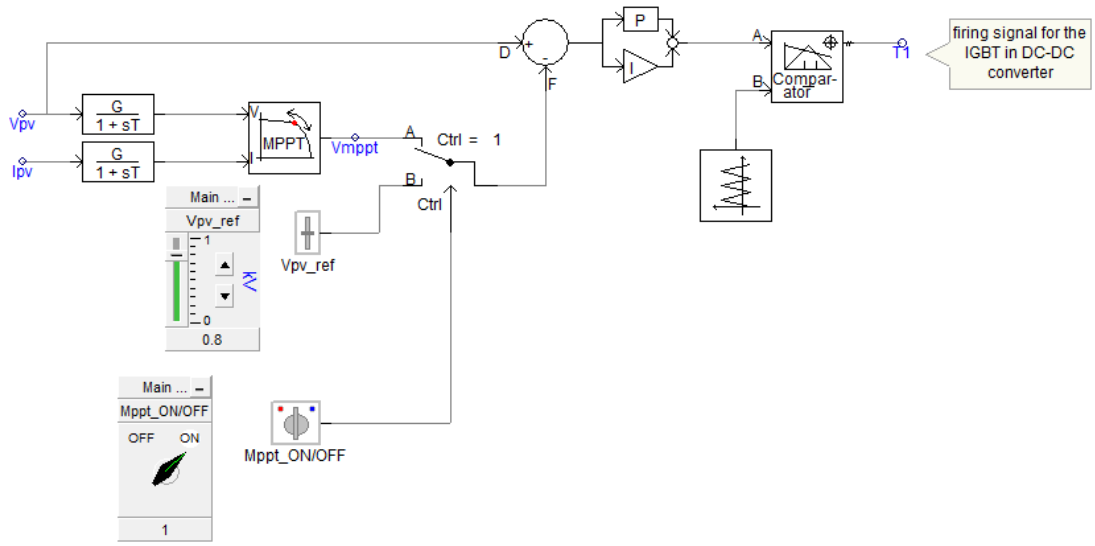

Figure 3.3: Firing signal generation to the DC-DC converter with MPPT

DC-DC converters are power electronic circuits that transform a DC voltage from one level to another level with minimum energy wastage. There are different types of DC-DC converters are listed in [28]. In this research study, DC-DC buck converter was selected to stepdown output voltages of PV array to the required input voltages to the inverter bridge (i.e. 400 V for the single phase and 800 V for the three phase inverter).

3.1.3. Parameter selection for the DC-DC buck converter

In this PSCAD models, DC-DC buck converter was designed by following the calculation steps with generalized assumptions as explained in [29].

For the buck converter shown in Figure 3.4, the inductance, input capacitance and output capacitance should be calculated. Then, the following calculation steps were used which were explained in the literature clearly.

V_{in} – Input voltage (high voltage to be converted)

V_{out} – Output voltage (converted low voltage)

I_{load} – Load current (rated current of the inverter)

f_{sw} – Switching frequency

L – Inductance

C_{in} – Input capacitance

C_{out} – Output capacitance

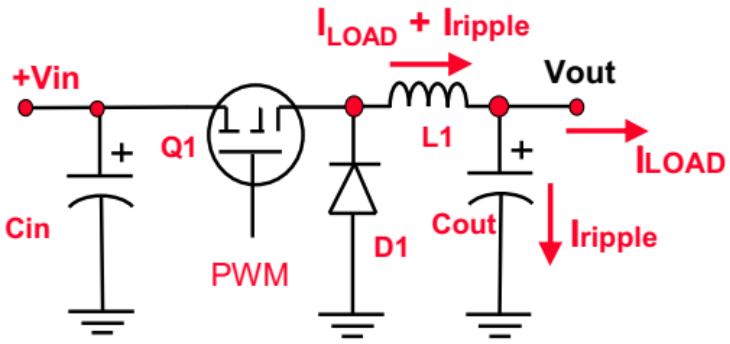

Figure 3.4: DC – DC buck converter circuit [29]

Considering typical output current ripple of 30%, the ripple current will be limited to 30% of maximum load.

Then,

$$\Delta I = 0.3 I_{load} \tag{3.1}$$

Starting from basic equations,

$$V = L\frac{di}{dt} \tag{3.2}$$

From Eqn. 3.2

$$L = V\frac{dt}{di} = V\frac{\Delta t}{\Delta I}$$

$$\text{The inductance, } L = \frac{(V_{in} - V_{out})\frac{V_{out}}{V_{in}}}{f_{SW} \cdot \Delta I} \tag{3.3}$$

Where,

$$\Delta t = \frac{V_{out}/V_{in}}{f_{sw}}$$

The voltage ripple across the output capacitor is the sum of ripple voltages due to the Effective Series Resistance (ESR) and due to the capacitor's Effect Series Inductance (ESL). For the output capacitor voltage ripple can be expressed as in Eqn. 3.4.

$$\Delta V = \Delta I \left(ESR + \frac{\Delta t}{C_{out}} + \frac{ESL}{\Delta t} \right) \tag{3.4}$$

For this case, we will assume that the ESL value is zero. If switching frequencies increase (>1 MHz), the ESL specification will become more important.

Then,

$$\Delta V = \Delta I \left(ESR + \frac{\Delta t}{C_{out}} \right) \quad (3.5)$$

The output capacitance, $C_{out} = \frac{\Delta I \cdot \Delta t}{\Delta V - (\Delta I \cdot ESR)}$ (3.6)

The desired output voltage ripple is defined as 50 mV. (i.e.$\Delta V = 0.05\ V$)

Assuming the power dissipation in the output capacitor is 0.01W, it can be written as in Eqn. 3.7.

$$\Delta I^2 \cdot ESR = 0.01 \quad (3.7)$$

The estimated input ripple current,

$$\Delta I_{in} \approx \frac{I_{load}}{2} \quad (3.8)$$

As same as the output capacitor, the input capacitor selection is primarily dictated by the ESR requirement needed to meet voltage ripple requirements. Usually, the input voltage ripple requirement is not as stringent as the output voltage ripple requirement. The input ripple current rating for the input capacitors may be the most important criteria for selecting the input capacitors. Often the input ripple current will exceed the output ripple current.

The input capacitance, $C_{in} = \frac{\Delta t}{\left(\frac{\Delta V_{in}}{\Delta I_{in}}\right) - ESR}$ (3.9)

In this case, the maximum input voltage ripple was defined as 200 mV (i.e.$\Delta V_{in} = 0.2\ V$). ESR can be calculated from Eqn. 3.10.

The estimated power dissipation in the input capacitor is 0.01 W,

$$\Delta {I_{in}}^2 \cdot ESR = 0.01 \quad (3.10)$$

3.1.4. Inverter

The DC to AC inversion is done by the inverter bridge. In this study, IGBTs were selected to develop the inverter bridges as IGBT has advantages of the other power switches like Metal Oxide Semiconductor Field Effect Transistor (MOSFET), Gate Turn Off thyristor (GTO) and Bipolar Junction Transistors (BJT) combined. Similar to MOSFET, it has high impedance gate which requires small amount of energy to

switch the device. Like BJT, it has a small on-state voltage even in devices with large blocking voltage ratings. IGBT can be designed to block negative voltages like GTO. IGBTs have turn-on and turn-off times on the order of 1 μs and are available in module ratings as large as 1.7 kV and 1.2 kA [30]. In this research study, IGBT switches were selected for inverter bridge modeling. Two pairs of IGBT switches are connected to form the H-bridge for the single phase inverter and three pairs of IGBT switches are connected to form three phase inverter bridge.

3.1.5. Inverter Controls

There are several PWM schemes which are used to pulse-width modulate the inverter switches in order to achieve the DC to AC inversion. In this research, SPWM scheme was selected as the switching technique of both single phase and three phase inverters. To produce a sinusoidal signal as the output of the inverter where the amplitude and the frequency are at required magnitudes, a sinusoidal reference (control) signal at the fundamental frequency is compared with a triangular signal at the switching frequency. Fundamental frequency component of the half-bridge inverter output can be stated as in Eqn. 3.11 and in phase with the reference signal. Peak amplitude of the fundamental component of the inverter output can be obtained as in Eqn. 3.12.

$$V_1 = \frac{\hat{V}_{ref}}{\hat{V}_{tri}} \sin \omega_1 t \cdot \frac{V_d}{2} \tag{3.11}$$

$$\hat{V}_1 = m_a \cdot \frac{V_d}{2} \tag{3.12}$$

Where,

$V_1 -$ fundamental component of the inverter output

$\hat{V}_1 -$ peak amplitude of the fundamental component

$\hat{V}_{ref} -$ peak amplitude of the reference signal

$\hat{V}_{tri} -$ peak amplitude of the triangular signal

$V_d -$ DC voltage

Eqn. 3.11 and 3.12 will be satisfied if the modulation is linear; $m_a \leq 1$(described in chap. 2). In this research, the power switches are operated by PWM with bipolar voltage switching. Therefore, in full-bridge inverter which has two pair of IGBT switches the diagonally opposite switches from two legs are switched as switch pairs

1 and 2 respectively. Hence, the peak of the fundamental component in the full-bridge inverter output can be determined by Eqn. 3.13

$$\widehat{V}_1 = m_a \cdot \frac{V_d}{2} \tag{3.13}$$

As stated in chap. 2, m_f was selected to be an odd integer to mitigate the harmonic production of the inverters. Therefore, the switching frequency was 6.25 kHz which was chosen to comply with the constraints explained in [15]. The system frequency is 50 Hz.

3.1.6. LCL Filter

Number of filter networks suitable for PV systems are discussed in the literature. Among mostly used three passive filter networks of L, LC and LCL, the LCL filter was chosen for this model as it possesses better filtering effects such as less current ripple, low reactive power production, good decoupling between filter and the grid impedance and higher attenuation at resonance frequency [31-33]. As LCL filter possesses the highest attenuation of 60 dB/decade for the frequencies above its resonant frequency, it is very much important to set its cut-off frequency precisely to comply with the constraint (3.14).

$$10f_g \leq f_{res} \leq 0.5f_{sw} \tag{3.14}$$

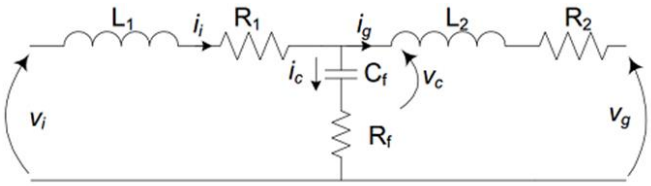

Figure 3.5: LCL Filter Circuit [8]

From Figure 3.5 which displays the LCL filter circuit,

L_1 – inverter side inductance

R_1 – inverter side inductor resistance

L_2 – grid side inductance

R_2 – grid side inductor resistance

C_f – filter capacitance

R_f – damping resistance

These filter parameters were calculated by following a mostly used algorithm; described as follows.

By considering, rated quantities of the inverter

E_n – inverter output RMS voltage

P_n – rated active power

V_{dc} - DC voltage

f_g – fundamental frequency

f_{sw} – switching frequency

And defined quantities;

Z_b – base impedance

C_b – base capacitance

Calculating base impedance,

$$Z_b = \frac{{E_n}^2}{P_n} \tag{3.15}$$

Then,

$$\text{The base capacitance, } C_b = \frac{1}{\omega_g Z_b} \tag{3.16}$$

Filter parameters are referred to percentage of base values. For the design of filter capacitance (C_f)

By considering the maximum power factor variation seen by the grid = 5%

Then, the design factor of filter capacitance = 5%

Therefore,

$$C_f = 0.05 C_b \tag{3.17}$$

Let the maximum current ripple at the inverter output be ΔI_{Lmax},

$$\Delta I_{Lmax} = \frac{2V_{dc}(1-m_a)m_a T_{sw}}{3L_1} \tag{3.18}$$

Where m_a is the amplitude modulation index of the inverter (as explained in inverter controls)

By considering 10% of current ripple of the rated current;

$$\Delta I_{Lmax} = 0.1\ I_{max} \tag{3.19}$$

$$I_{max} = \frac{P_n\sqrt{2}}{3V_{ph}} \tag{3.20}$$

LCL filter should reduce the expected current ripple to 20%

Then, it results in a current ripple value at the inverter output=2%

To calculate current ripple reduction,

After analyzing the filter circuit and considering it as a current source,

$$\frac{i_g(h)}{i_i(h)} = \frac{1}{|1+r[1-L_1 C_b \omega_{SW}^2 x]|} = k_a \quad (3.21)$$

Where,

$$r = \frac{L_1}{L_2}$$

$x =$ maximum power factor variation seen by the grid(0.05)

In this case, $k_a = 0.2$

Then,

$$L_2 = \frac{\sqrt{\frac{1}{k_a^2}}+1}{C_f W_{sw}^2} = \frac{6}{C_f W_{sw}^2} \quad (3.22)$$

Resonance frequency,

$$\omega_{res} = \sqrt{\frac{L_1+L_2}{L_1 L_2 C_f}} \quad (3.23)$$

To attenuate the ripple on the switching frequency

Damping resistance = $\frac{1}{3}$ of filter capacitance impedance at ω_{res}

$$R_f = \frac{1}{3\omega_{res} C_f} \quad (3.24)$$

Table 3.2 gives the LCL filter parameters of 2 kW single phase and three phase inverters.

Table 3.2: LCL Filter Parameters

Inverter Type	**Single Phase**	**Three Phase**
Inverter side Inductance (H)	0.0046	0.026
Grid side inductance (H)	0.0007	0.002
Filter capacitance (μF)	5.5200	2.000
Damping resistance (Ω)	3.5000	10.00

3.1.7. RLC Tuned Filter

In addition to the LCL filter, RLC filter was designed as presented in Figure 3.6 only for single phase inverters to mitigate the harmonics at switching frequency and its bands further.

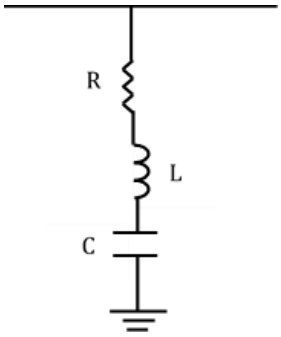

Figure 3.6: RLC Filter Circuit

$$Z = R + j\omega L + \frac{1}{j\omega C} = R + j\left(\omega L - \frac{1}{\omega C}\right) \quad (3.25)$$

At resonant frequency, Z is real;

$$\omega_0 = \sqrt{\frac{1}{LC}} \quad (3.26)$$

At cutoff frequencies,

$$I = \frac{1}{\sqrt{2}} I_{peak} \; ; \; I_{peak} = \frac{V}{R} \quad (3.27)$$

Then,

$$\omega = \pm\frac{R}{2L} + \sqrt{\left(\frac{R}{2L}\right)^2 + \frac{1}{LC}} \quad (3.28)$$

Parameters are assigned to fulfill the required filtering and the desired cut-off frequencies are as follows.

Lower cut-off frequency (ω_1) = 12000π rads^{-1}

Upper cut-off frequency (ω_2) = 13500π rads^{-1}

Resonant frequency (ω_0) = 12500π rads^{-1}

Then,

Bandwidth = $\omega_2 - \omega_1 = \frac{R}{L} = 4.712 \times 10^3$

$$\omega_0 = \sqrt{\frac{1}{LC}} = 6.484 \times 10^{-10}$$

Let R= 1 Ω for the simplicity

Then,

$L = 0.2122$ mH

$C = 3.055\mu F$

3.1.8. PSCAD Models and Inverter Performances

Figure 3.7 and 3.8 present the PSCAD models of three phase and single phase PV systems respectively, including all the components described above. In detailed modeling both three phase and single phase inverters are designed to be operated at the same capacity of 2 kVar.

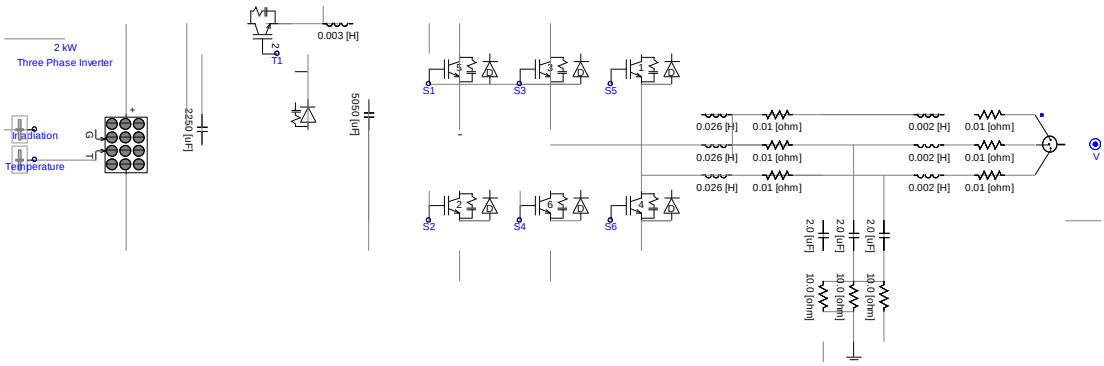

Figure 3.7: PSCAD Model of three phase inverter

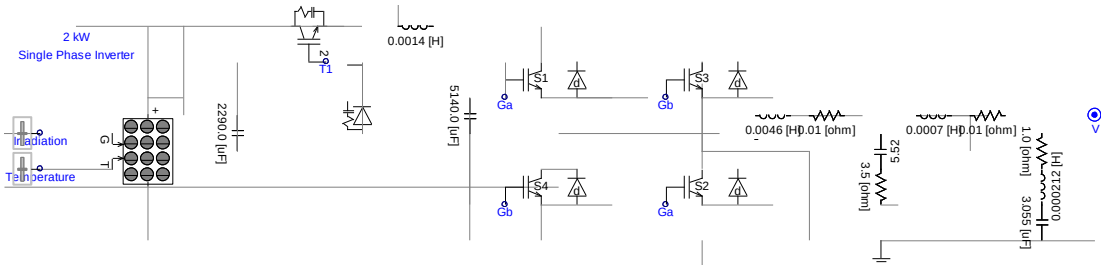

Figure 3.8: PSCAD Model of single phase inverter

Filtered output waveforms of voltage and current of the single phase inverter are displayed in Figure 3.9 and 3.10.

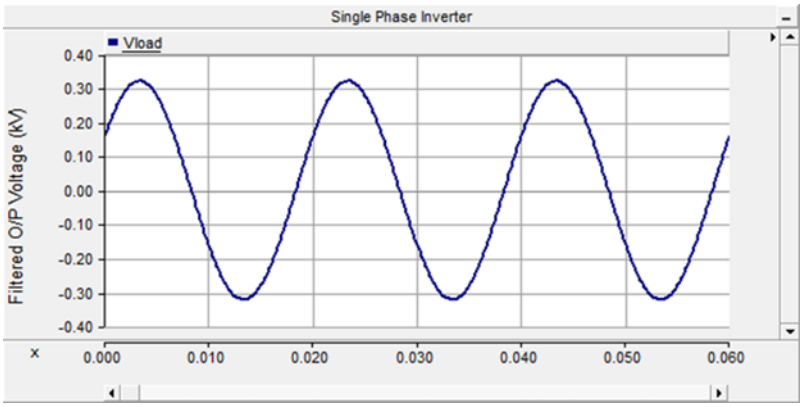

Figure 3.9: Output voltage waveform of the single phase inverter

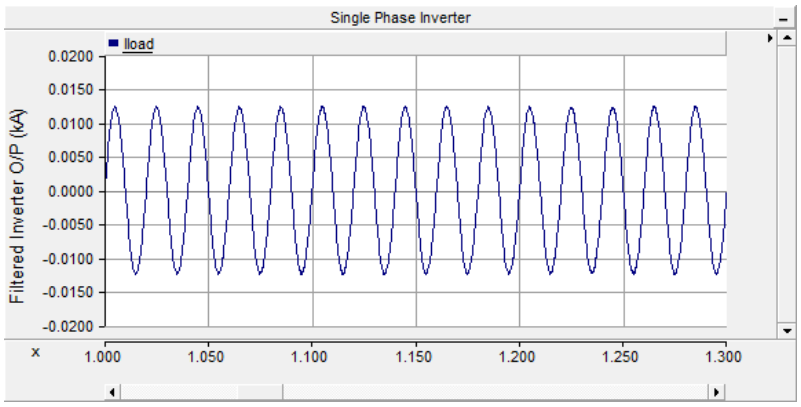

Figure 3.10: Filtered current waveform of the single phase inverter

Filtered output waveforms of voltage and current of the three phase inverter are displayed in Figure 3.11 and 3.12.

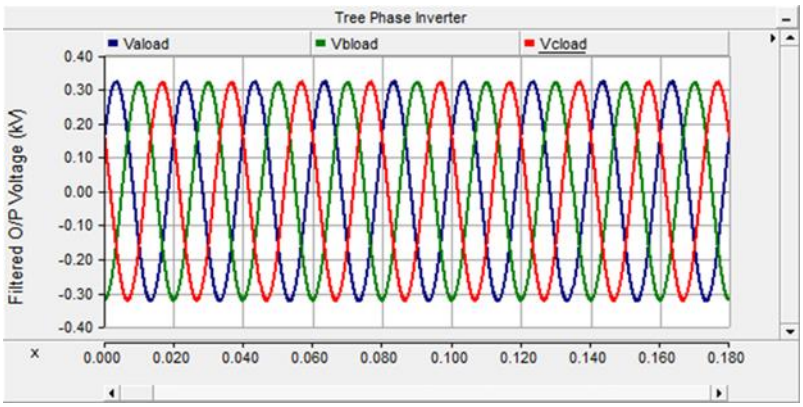

Figure 3.11: Output voltage waveforms of the three phase inverter

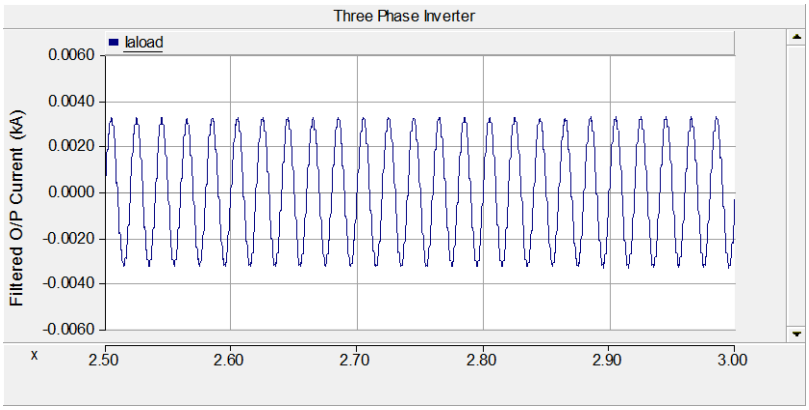

Figure 3.12: Filtered phase A current waveform of the three phase inverter

3.2. Network Modeling

The entire power system is consisted with three main categories such as generation, transmission and distribution. About 75% of daily electricity generation is owned by Ceylon Electricity Board (CEB) while the balance of 25% is contributed by Independent Power Producers (IPPs), Small Power Producers (SPPs) and other renewable projects [34]. The transmission system comprises 220 kV and 132 kV transmission lines interconnecting grid substations and power stations. The distribution is controlled by both CEB at voltage levels 33 kV, 11 kV and 400 V and Lanka Electricity Company (private) limited (LECO) at voltage levels 11 kV and 400 V only. The total length of distribution lines is 165540 km by year 2015 including overhead lines and underground cables [35][36]. LECO operates the distribution in the western coastal belt of the island from Negombo to Galle. LECO distribution network is connected to the 33 kV medium voltage distribution network through the distribution utilities of CEB. LECO distribution network also consists of overhead lines and underground cables which are designed as interconnected set of radial feeders [37].

Currently, high solar PV penetration has been reported in Kotte area. Required technical information of the distribution transformer (AZ0202 in Appendix A) such as transformer data, number of feeders and load distribution is available as the network has been organized well for research studies. Therefore, one of the existing distribution feeder of AZ0202 from Pitakotte branch area was selected for the network modeling. Solar PV integrations were planned to do as depicted in Figure 3.13.

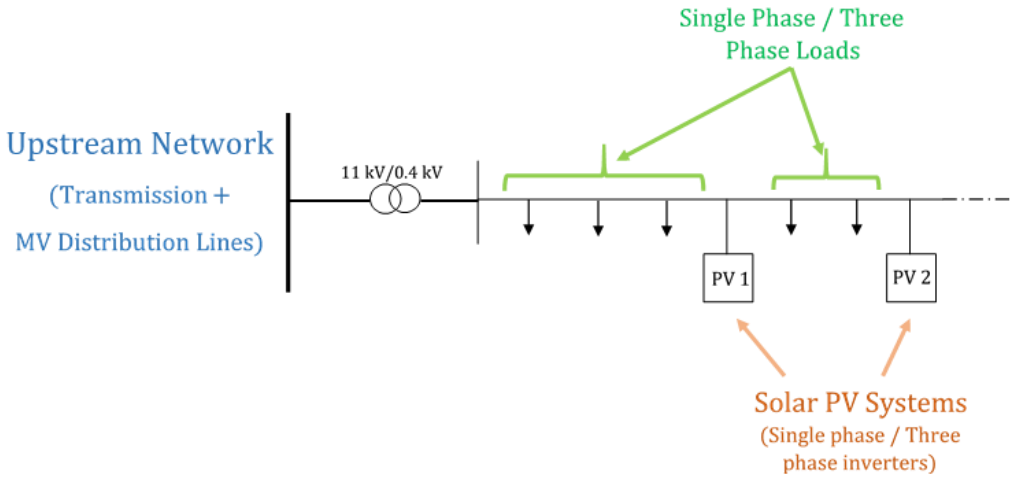

Figure 3.13: Planned solar PV integrations in LV distribution network

3.2.1. Upstream network representation

Three phase voltage source is used to represent the upstream utility grid. Considering some existing fault levels at Primary Sub Stations (PSS), three different values were estimated to differentiate the network as strong, intermediate and weak. Allowing for the worst situation, weak network was selected and respective impedance was added to the network to gain the real network performance. Figure 3.14 provides the PSCAD modeling of equivalent upstream utility grid representation. The values, 50 Hz for the system frequency and 11 kV for the line-to-line rms voltage at the output of voltage source are set as input parameters.

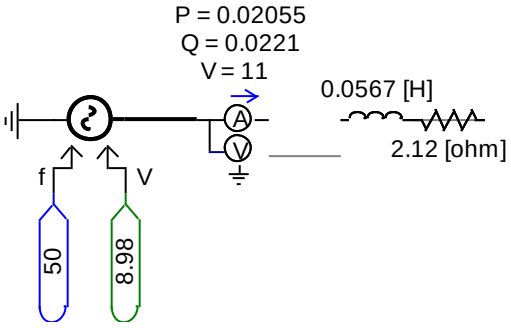

Figure 3.14: PSCAD model of upstream utility grid

3.2.2. Transformer

An 11 kV/ 400 V stepdown transformer (labeled as AZ0202 in Appendix A) was modeled as in Figure 3.15 (a). Transformer parameters are displayed in Figure 3.15(b).

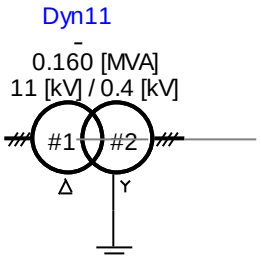

(a)

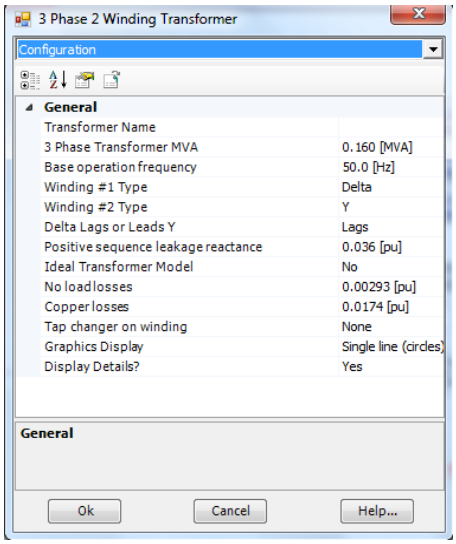

(b)

Figure 3.15: Transformer modeling

3.2.3 Distribution Line and Load Modeling

Power distribution path from the distribution transformer to consumers is depicted as in Figure 3.16. In distribution line modelling, the impedances of FDS and T-OFF piercing connectors are neglected. Aerial Bundled Cables (ABC) are used as overhead feeders to distribute power to the residential premises.

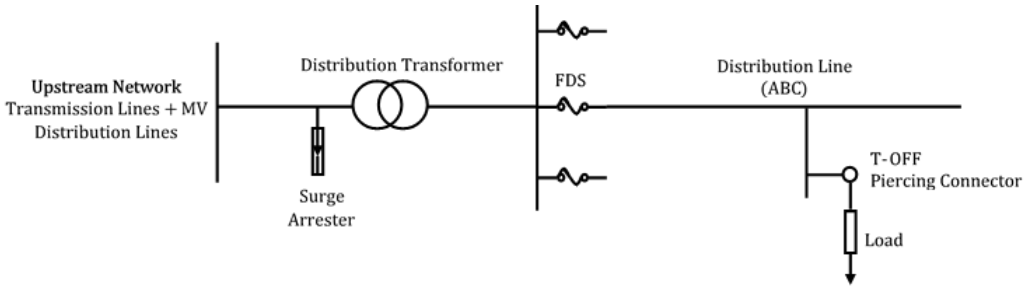

Figure 3.16: OH distribution line configuration of a practical feeder

Technical information (i.e. resistance and inductance) of ABC are used for calculations as in Table 3.3. Load distribution data of the selected feeder as at the year 2015 are tabulated in Table 3.4.

Table 3.3: Technical information of ABC

Nominal area of the conductor (mm^2)	Resistance (Ω/km)	Inductance (mH/km)
50	0.64	0.27

All the services from each pole were modeled as constant three phase power loads with After Diversity Maximum Demand (ADMD) approach as expressed in Eqn. 3.35 [38][39]. Power factor 0.9 is applied to all loads. This work considers steady state voltage and current and these loads behave as linear loads. Hence zero background harmonics.

$$\mathrm{ADMD} = \lim_{N\to\infty} \frac{1}{N} \sum_{n=1}^{N} D_n \qquad (3.35)$$

Where,

ADMD = After Diversity Maximum Demand per customer

N = Number of customers

D_n = Demand of customer n at the time of system maximum demand

Traditionally, Active power component (P) and reactive power component (Q) of any type of load model with their voltage dependency can be expressed in exponential form as in Eqn. 3.36 and Eqn. 3.37 [40].

$$P(V) = P_0 \left(\frac{V}{V_0}\right)^a \quad (3.36)$$

$$Q(V) = Q_0 \left(\frac{V}{V_0}\right)^b \quad (3.37)$$

Where,

V = magnitude of the bus voltage

P_0, Q_0 and V_0 = respective variables at initial operating condition

a = b = 0, 1, 2 respectively for constant power, constant current and constant impedance characteristic models

The exponents a and b are nearly equal to the slope of dP/dV (dQ/dV) at $V = V_0$.

Table 3.4: Load distribution in Feeder 2

Feeder Name	F2			
ADMD(KVA)	0.38			
Power Factor	0.90			
Pole Name		Cable type	Pole Span (m)	No. of Services
F2		**ABC 50**		
	EN6		27	16
	EN7		33	13
	EN7-1		22	1
	EN8		18	4
F2-1		**ABC 50**		
	EN7/1		38	6
	EN7/2		14	3
	EN7/3		31	3
	EN7/4		36	5
	EN7/5		30	5
	EN7/6		23	8
	EN7/7		43	6
	EN7/8		9	8
	EN7/9		11	2
	EN7/10		22	8
F2-2		**ABC 50**		
	EN8/1		2	14
	EN8/2		24	0
	EN8/3		29	13

4. HARMONIC INJECTIONS DUE TO DIFFERENT SOLAR PV CONFIGURATIONS: Analysis of Simulation Results

Three number of three phase (labeled as T1, T2 and T3) and three number of single phase (labeled as S1, S2 and S3) inverters were connected to six different selected points at feeder 2 and operated under Standard Test Conditions (STC) (i.e. 1000 W/m^2 and 25 ^{0}C) as shown in Figure 4.1. These six points were chosen to evaluate the harmonic propagation of each inverter in their individual operation and multiple operation. The following six different locations of the feeder were selected to measure the THD with different PV integrations to represent beginning of a distribution feeder, intermediate and the end of the feeder.

Location 1 – at the secondary of the transformer

Location 2 – at the 400 V bus

Location 3 – at the beginning of Feeder 2-2 (F2-2)

Location 4 – near the POC of T2

Location 5 – at the beginning of Feeder 2-1 (F2-1)

Location 6 – near the POC of S3

The range of power factor of the solar PV system shall be from 0.9 lagging to 0.9 leading [9]. All six inverters of this case study are working within this range.

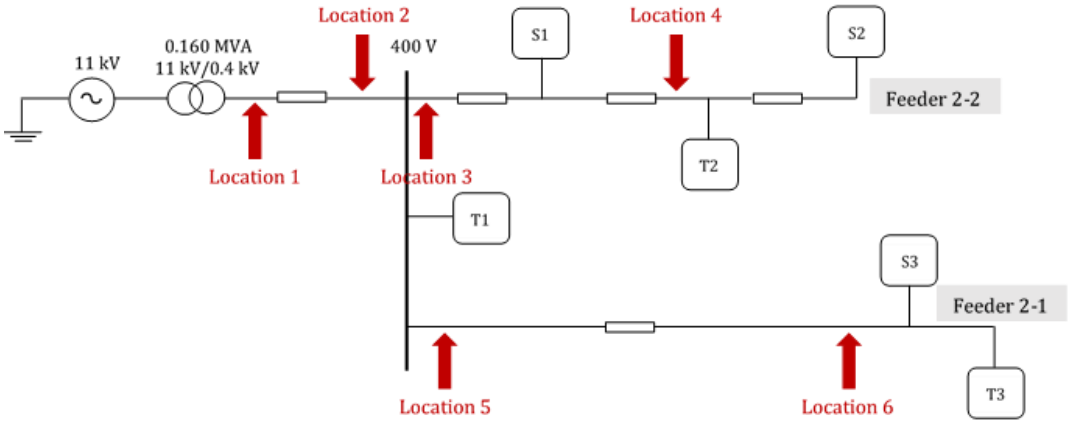

Figure 4.1: Schematic of the complete system with PV integrations

Loads in the distribution feeder behave as linear loads. Therefore, the background harmonic distortion is zero.

Four number of scenarios were followed as described below to study the harmonic generation and their impact.

Scenario 1

Case 1 - Only one single phase inverter (S1) is connected to the grid (Figure 4.2 (a))

Case 2 - All three number of single phase inverters (S1, S2 and S3) are connected (Figure 4.2 (b))

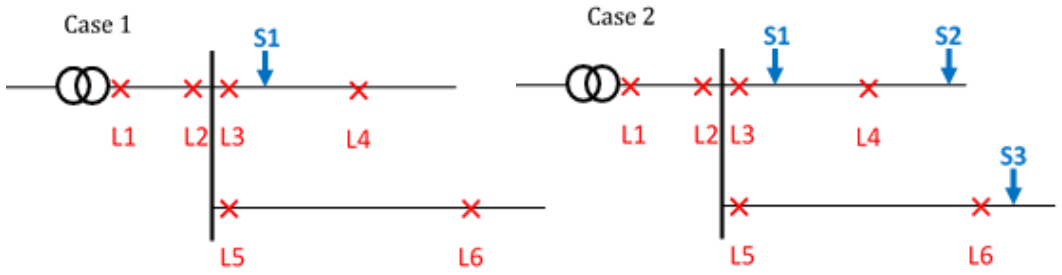

(a) (b)

Figure 4.2: Schematic of scenario 1

Scenario 2

Case 1 - Only one three phase inverter (T1) is connected to the grid (Figure 4.3 (a))

Case 2 - All three number of three phase inverters (T1, T2 and T3) are connected (Figure 4.3(b))

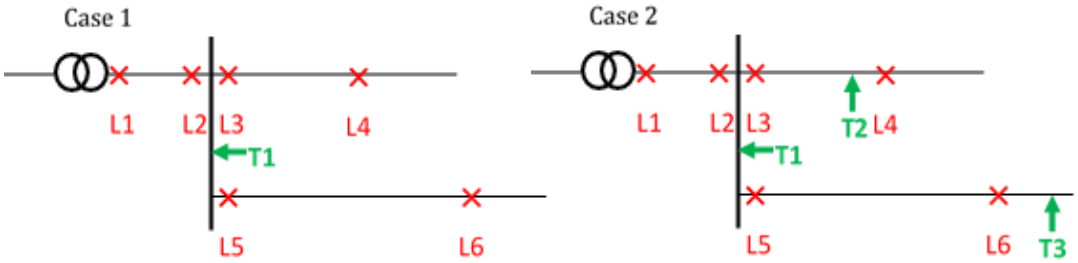

(a) (b)

Figure 4.3: Schematic of scenario 2

Scenario 3

Case 1 - All six inverters (S1, S2,…. T3) are connected; 60% of PV penetration (Figure 4.4 (a))

Case 2 - F2-2 inverters (S1, T1 and S2) are connected; 50% of PV penetration (Figure 4.4 (b))

Case 3 - F2-1 inverters (S3 and T3) are connected; 20% of PV penetration (Figure 4.4 (c))

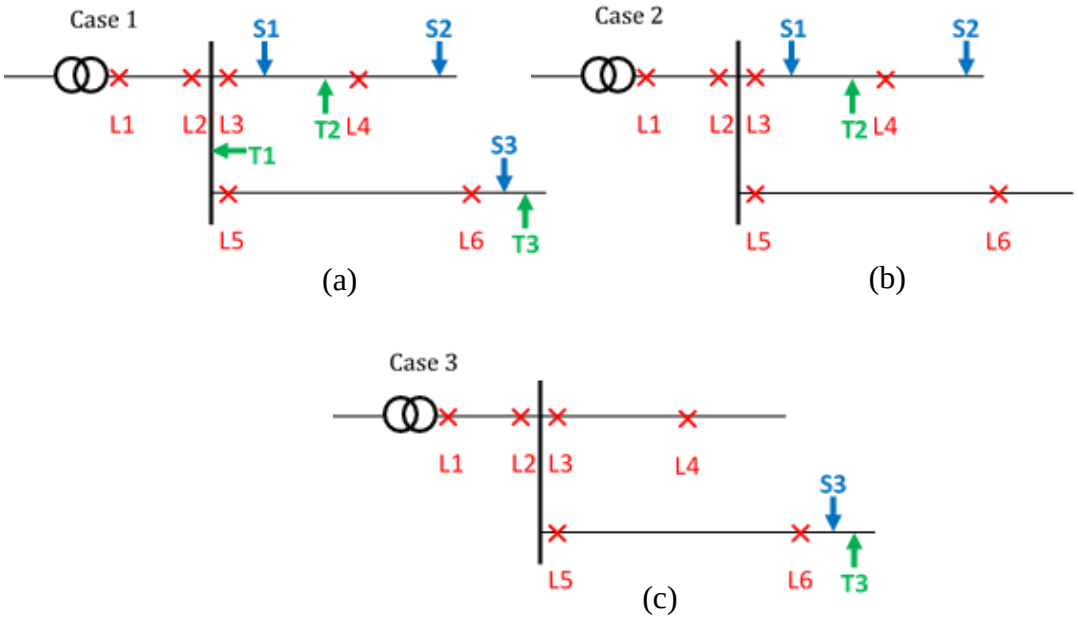

Figure 4.4: Schematic of scenario 3

Scenario 4

50% reduction of solar irradiance from its STC value

4.1. Inverter harmonics

Individual harmonic components of both voltage and current were measured at the single phase and three phase inverter outputs.

From Scenario 1 and Scenario 2,

Case 1 – one single phase/three phase inverter (S1) is connected to the grid

Case 2 – all single phase/three phase inverters are connected to the grid

The m_f of both single phase and three phase inverters is 125 which is an odd integer. Therefore, no sub-harmonics and no even-harmonics are appeared in the individual harmonic spectrum.

Significant individual harmonics which were present at the single phase inverter (S1) output are given in Table 4.1. Among all these individual harmonic magnitudes 3rd order harmonic is most dominant. With comparison of case 1 and case 2 individual harmonics, it is clear that some of them are attenuated in multiple operation.

Table 4.1: Individual harmonic magnitudes at S1 inverter output in Scenario 1

Harmonic order (h)	Magnitude			
	Case 1		Case 2	
	Amperes (A)	Percentage of fundamental (%)	Amperes (A)	Percentage of fundamental (%)
3	0.13	1.53	0.12	1.44
5	0.03	0.31	0.03	0.36
7	0.02	0.27	0.01	0.14
123	0.03	0.35	0.01	0.17
125	0.08	0.98	0.04	0.49
127	0.02	0.29	0.01	0.15

Similarly, above two cases were followed by the three phase inverters too. Lower percentage value of THD (THD%) was occurred at the three phase inverter output than the single phase inverter as the Individual Harmonic Distortion (IHD) of most dominant harmonics are cancelled out in the harmonic spectrum. Harmonic generation of single phase h-bridge inverter and the three phase inverter can be explained as follows;

Considering Figure 4.5 (a), the output voltage of the full-bridge inverter ($V_{ab}(t)$) can be written as in (4.1)

$$V_{ab}(t) = V_{ao}(t) - V_{bo}(t) \quad (4.1)$$

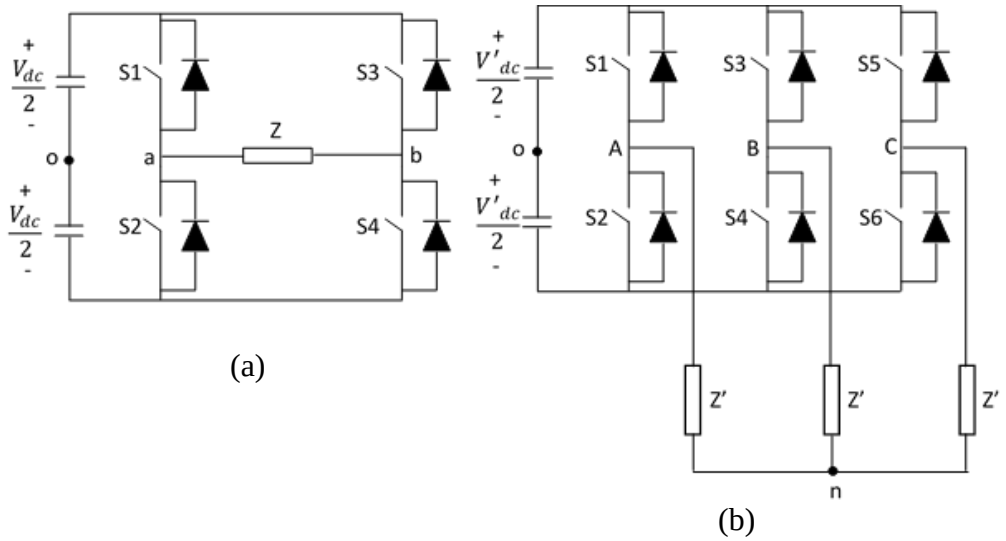

Figure 4.5: Schematics of single phase and three phase inverters

By considering one pair of IGBT switches S1 and S3, there are four switching combinations. $V_{ab}(t)$ varies with respect to the leg voltages of $V_{ao}(t)$ and $V_{bo}(t)$ as given in Table 4.2. In bi-polar modulation, the inverter output voltage is a square wave which varies between $-V_{dc}$ and $+V_{dc}$ as shown in Figure 4.6.

Table 4.2: Voltage at the output of the single phase inverter bridge

S1	S3	$V_{ao}(t)$	$V_{bo}(t)$	$V_{ab}(t)$
0	0	$\frac{-V_{dc}}{2}$	$\frac{-V_{dc}}{2}$	0
0	1	$\frac{-V_{dc}}{2}$	$\frac{+V_{dc}}{2}$	$-V_{dc}$
1	0	$\frac{+V_{dc}}{2}$	$\frac{-V_{dc}}{2}$	$+V_{dc}$
1	1	$\frac{+V_{dc}}{2}$	$\frac{+V_{dc}}{2}$	0

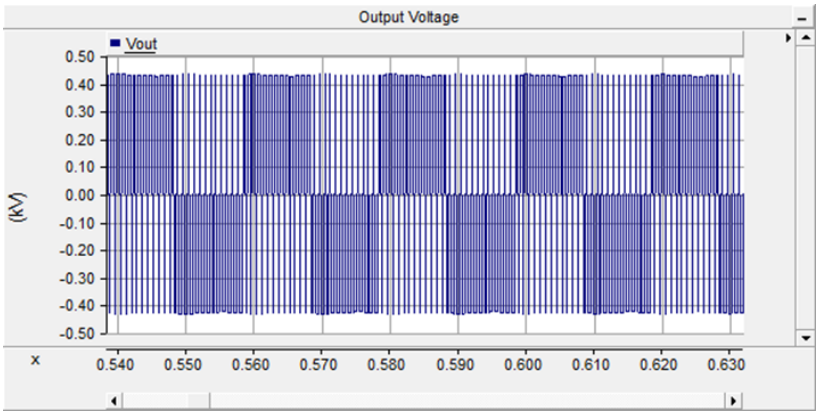

Figure 4.6: Voltage waveform at the inverter bridge output

From Figure 4.5 (b), Phase voltages of three phase inverter $V_{An}(t)$, $V_{Bn}(t)$ and $V_{Cn}(t)$ can be expressed as follows.

$$V_{An}(t) = V_{Ao}(t) - V_{no}(t) \quad (4.2)$$

$$V_{Bn}(t) = V_{Bo}(t) - V_{no}(t) \quad (4.3)$$

$$V_{Cn}(t) = V_{Co}(t) - V_{no}(t) \quad (4.4)$$

$$V_{no}(t) = \frac{V_{Ao}(t)+V_{Bo}(t)+V_{Co}(t)}{3} \quad (4.5)$$

Where, $V_{Ao}(t)$, $V_{Bo}(t)$ and $V_{Co}(t)$ are leg voltages and $V_{no}(t)$ is common node voltage. Table 4.3 gives the variation of the Phase A voltage with IGBT switching patterns. Output voltage signal possesses the odd symmetry as the m_f is an odd integer in this study. Therefore, coefficients of the cosine series are zero of the Fourier series representation of the voltage signal. Fourier series representation of a non-sinusoidal waveform can be expressed as follows.

$$f(t) = F_0 + \sum_{h=1}^{\infty} f_h(t) = A_0 + \sum_{h=1}^{\infty}\{A_h \cos h\omega t + B_h \sin h\omega t\} \quad (4.6)$$

$A_0 = A_h = 0$ (For odd symmetric waveforms and no dc component)

Then, Current at the inverter output with a balanced load is given by Eqn. 4.7.

$$I_{An}(t) = \frac{V_{An}(t)}{Z'} = \frac{\sum_{h=1}^{\infty}\{B_h \sin(h\omega t+\theta)\}}{Z'} \quad (4.7)$$

Then, Harmonic magnitudes of odd symmetric waveform will be

$$F_h = \frac{B_h}{\sqrt{2}} \quad (4.8)$$

Table 4.3: Voltage of a single phase at the three phase inverter bridge output

S1	S3	S5	$V_{Ao}(t)$	$V_{no}(t)$	$V_{An}(t)$
0	0	0	$-\frac{V'_{dc}}{2}$	$-\frac{V'_{dc}}{2}$	0
0	0	1	$-\frac{V'_{dc}}{2}$	$-\frac{V'_{dc}}{6}$	$-\frac{V'_{dc}}{3}$
0	1	0	$-\frac{V'_{dc}}{2}$	$-\frac{V'_{dc}}{6}$	$-\frac{V'_{dc}}{3}$
0	1	1	$-\frac{V'_{dc}}{2}$	$+\frac{V'_{dc}}{6}$	$-\frac{2V'_{dc}}{3}$
1	0	0	$+\frac{V'_{dc}}{2}$	$-\frac{V'_{dc}}{2}$	$+\frac{2V'_{dc}}{2}$
1	0	1	$+\frac{V'_{dc}}{2}$	$+\frac{V'_{dc}}{6}$	$+\frac{V'_{dc}}{3}$
1	1	0	$+\frac{V'_{dc}}{2}$	$+\frac{V'_{dc}}{6}$	$+\frac{V'_{dc}}{3}$
1	1	1	$+\frac{V'_{dc}}{2}$	$+\frac{V'_{dc}}{6}$	0

Further, the waveform of phase voltage signal can be explained with Figure 4.7.

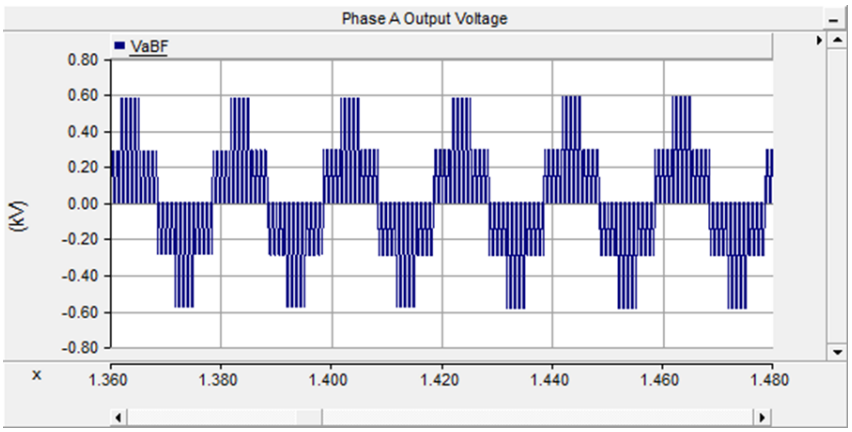

Figure 4.7: Phase A voltage signal at three phase inverter bridge output

Harmonic magnitudes depend on the value of f (t) at particular time period. Three phase inverter produces a phase voltage which is more near the sinusoidal ac voltage than the single phase inverter. Then, the harmonic production of three phase inverters is less than single phase inverters.

4.2. Total Harmonic Distortion of Voltage and Current in single phase inverter integrations

Percentage value of V_{THD} and I_{THD} (V_{THD} % and I_{THD} %) were measured at the single phase inverter outputs with different combinations of inverters S1, S2 and S3. The results are tabulated in Table 4.4.

Table 4.4: THD% at the outputs of single phase inverters

Inverter in operation			S1		S2		S3	
Distance from the transformer (m)			82		155		317	
S1	S2	S3	V_{THD}%	I_{THD}%	V_{THD}%	I_{THD}%	V_{THD}%	I_{THD}%
1			0.14	1.99				
	1				0.15	1.89		
		1					0.16	1.93
1	1		0.16	1.63	0.17	1.54		
	1	1			0.16	1.72	0.17	1.52
1		1	0.15	1.79			0.18	1.50
1	1	1	0.18	1.68	0.19	1.65	0.19	1.67

These results prove that the attenuation of individual current harmonics as the THD% are reduced in multiple operation. In individual operation of single phase inverters, V_{THD}% is increased slightly with the distance of the POC from the distribution transformer.

4.3. Total Harmonic Distortion of voltage and current in three phase inverter integrations

Table 4.5 gives V_{THD}% and I_{THD}% at three phase inverter outputs with different inverter operations. As same as single phase inverters minor V_{THD}% increment is observed. But, V_{THD}% s are less than single phase inverters. The grid impedance causes the V_{THD}% to be increased as the POC is away from the distribution transformer can be theoretically explained with the aid of Figure 4.8 that provides generalized equivalent circuit of a utility grid with solar PV integrations.

Table 4.5: THD% at the outputs of three phase inverters

Inverter in operation			T1		T2		T3	
Distance from the transformer (m)			60		102		317	
T1	T2	T3	V_{THD}%	I_{THD}%	V_{THD}%	I_{THD}%	V_{THD}%	I_{THD}%
1			0.03	1.18				
	1				0.04	1.18		
		1					0.05	1.16
1	1		0.06	1.12	0.07	1.11		
	1	1			0.07	1.14	0.08	1.06
1		1	0.06	1.12			0.08	1.06
1	1	1	0.09	1.13	0.10	1.07	0.11	1.10

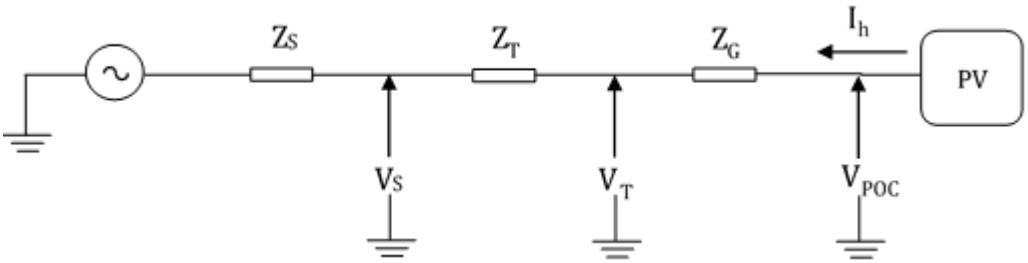

Figure 4.8: Diagram of a grid connected PV system

Z_S – Source impedance

Z_T – Transformer impedance

Z_G – Resultant grid impedance from the distribution transformer to the POC

Let, Z_h – impedance at h^{th} harmonic frequency

V_h – Harmonic voltage at h^{th} harmonic

I_h – harmonic current at h^{th} harmonic

From Ohm's Law h^{th} harmonic voltage can be written as,

$$V_h = I_h \times Z_h \quad (4.9)$$

At POC, h^{th} harmonic voltage is

$$(V_{POC})_h = I_h \times (Z_{Gh} + Z_{Th} + Z_{Sh}) \quad (4.10)$$

At source, hth harmonic voltage is

$$(V_S)_h = I_h \times Z_{Sh} \quad (4.11)$$

Hence,

$$(V_S)_h < (V_{POC})_h \quad (4.12)$$

For the same harmonic frequency, the voltage harmonic magnitude $(V_{POC})_h$ is increased with the distance from the distribution transformer.

THD% is highly affected by the fundamental value of the waveform as the THD% is a percentage of the fundamental (refer Eqn. 2.2). In this study, the fundamental value of current in single phase inverter is greater than that of three phase inverter. Therefore, significant difference of I_{THD}% s cannot be observed between single phase and three phase inverter outputs despite the fact that three phase inverter produces less harmonic magnitudes.

4.4. Total Harmonic Distortion of voltage at six locations of the distribution feeder

Case 1 – The total six number of PV inverters are connected to the grid

THD% s were measured at six different locations of the distribution feeder and they are tabulated in Table 4.6. Clearly, the V_{THD}% is increased along the feeder due to the influence of the grid impedance as well as the increment of harmonic current injection towards the feeder end when the distance from the distribution transformer to the harmonic measuring location is increased. Figure 4.9 shows the change in V_{THD}% along the feeder branches Feeder 2-1 and Feeder 2-2.

Table 4.6: THD% at six different locations in Case 1

Location	Distance from the distribution transformer (m)	Fault Level (MVA)	V_{THD}%	I_{THD}%
1	0	4.4	0.84	2.69
2	60	2.1	0.97	3.78
3	60	2.1	0.97	29.84
4	102	1.6	1.02	9.02
5	60	2.1	0.97	1.45
6	295	0.7	1.12	4.98

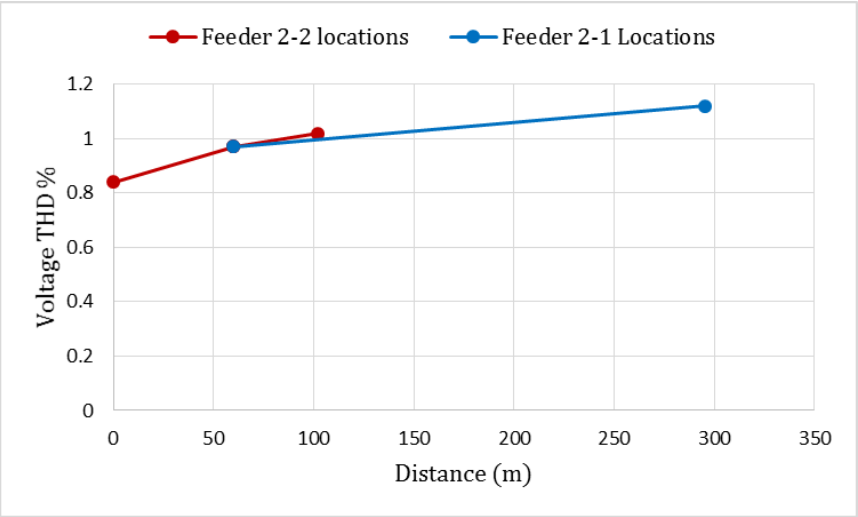

Figure 4.9: V_{THD}% variation along the feeders in Case 1

With PV integrations, the power flow is changed from its ordinary direction. Figure 4.10 presents the direction of the current flow in these six number of locations after the PV integrations.

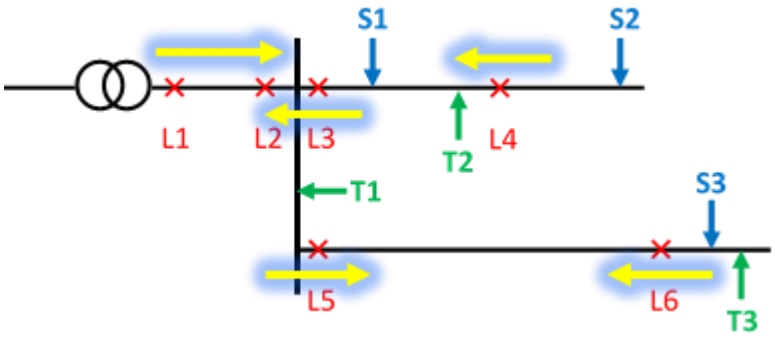

Figure 4.10: Current flow in selected six locations in Case 1

As shown in the figure 4.10, the current flow in location 3 is minimum. Therfore, the location 3 has the dominant I_{THD}% among all these locations. Even though the individual harmonics are equal in magnitudes, the percentage values are different and some of them violate the standard limitations as the fundamental currents are different in perticular locations.

Case 2 –The PV systems are connected to the feeder branch Feeder 2-2 only

There are three PV systems including one three phase inverter and two single phase inverters. The V_{THD}% and I_{THD}% were measured at the same six locations of the distribution feeder and given in Table 4.7.

Table 4.7: THD% at six different locations in Case 2

Location	V_{THD}%	I_{THD}%
1	0.64	1.12
2	0.74	1.55
3	0.74	30.03
4	0.80	9.29
5	0.74	0.65
6	0.73	0.65

The increasing pattern of V_{THD}% s is retained in case 2 also. But the percentage values are lowered as the PV integrations are reduced. The V_{THD}% at location 4 and 5 are almost constant. It implies that feeder 2-1 is not affected by the harmonics injected to the feeder 2-2. However, the supply voltage in feeder 2-1 is distorted than the situation which has no PV integrations. It is clearly shown in Figure 4.11. In this study, THD% s only in phase A were observed as S1, S2 and S3 are connected to the phase A in the distribution network.

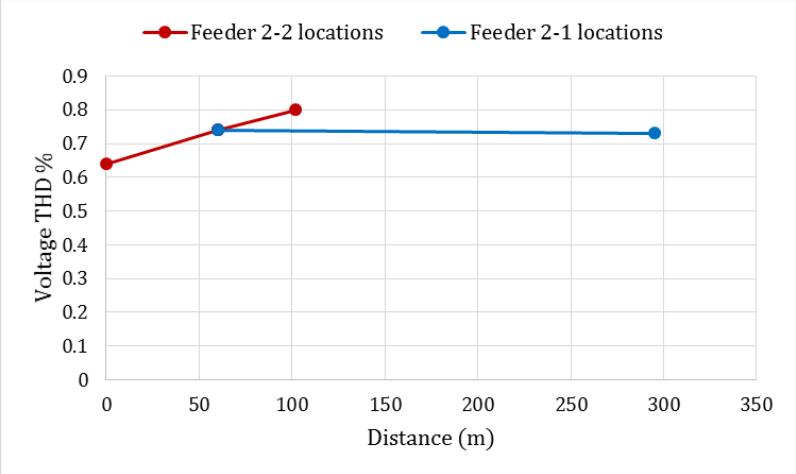

Figure 4.11: V_{THD}% variation along the feeder in Case 2

In this case, I_{THD}% at location 3 is higher than the other affected locations 1, 2 and 4. When all three inverters (i.e.S1, S2 and T1) are in operation, the excessive power flows towards the 400 V bus at the locations 3 and 4. Therefore, the fundamental current (rms current excepting harmonics) at the location 3 is the lowest. Hence, the highest I_{THD}%.

Case 3 –The PV systems are connected to the feeder branch Feeder 2-1 only

Two PV inverters (one single phase inverter and one three phase inverter) are connected to the feeder 2-1. Table 4.8 shows the V_{THD} % and I_{THD} % which were measured at six different locations.

Table 4.8: THD% at six different locations in Case 3

Location	V_{THD}%	I_{THD}%
1	0.33	0.44
2	0.38	0.54
3	0.38	0.34
4	0.38	0.34
5	0.38	1.33
6	0.60	5.05

V_{THD}% and I_{THD}% values are constant at the locations in Feeder 2-2 branch. They were not affected by connecting PV inverters to the other branch (i.e. Feeder 2-1). A similar observation as in case 2, a distortion in voltage and current is counted in Feeder 2-1 although no PV is connected to the same branch. Location 6 which is near the POC of both S3 and T3 has the highest V_{THD}% and I_{THD}%. At the location 6, the power flows towards the 400 V bus. The current flowing in location 6 is greater than that of in case 2 at location 3. Therefore, less I_{THD}% was occurred at location 6 than the I_{THD}% at location 3 in case 2, yet it is the dominant. The variation of V_{THD}% is shown in Figure 4.12.

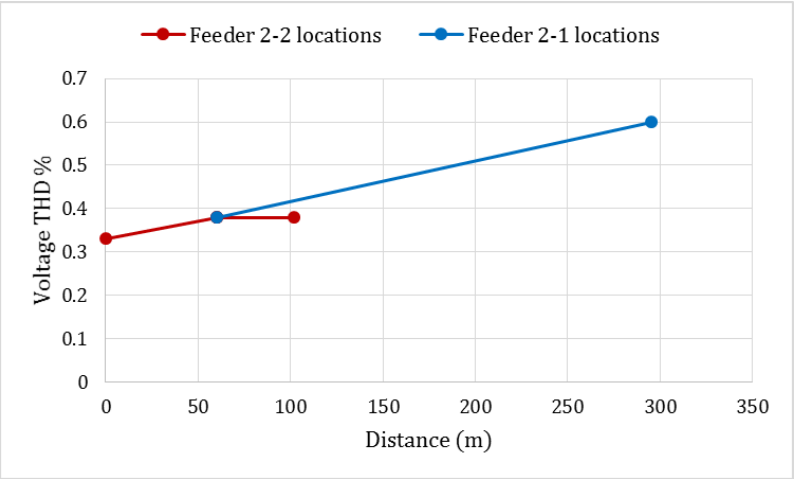

Figure 4.12: V_{THD}% variation along the feeder in Case 3

4.5. Effect of Solar Irradiance on Total Harmonic Distortion at Inverter Output

Solar irradiance was reduced to 500 W/m^2 (50% shading) and ambient temperature was maintained at its STC value of 25^{0}C. Then, V_{THD} % and I_{THD} % were measured at the output of single phase inverter (S1) and three phase inverter (T1). The readings are given in Table 4.9. THD % s show that an increment in harmonic distortion at the inverter outputs. But, there is no significant change in individual harmonic magnitudes. Though the voltage is maintained at its maximum power point, the power produced by the PV array is lowered (approximately 50 % reduction). Then the active power injected by the inverter was reduced. Accordingly, output current was lowered. As THD% is dependent on fundamental value of the voltage or current, low solar irradiance produces higher THD% than that of at STC values.

Table 4.9: THD% at inverter outputs of S1 and T1

Inverter Type	V_{THD}%		I_{THD}%	
	STC	50% shading	STC	50% shading
S1	0.14	0.13	1.99	2.94
T1	0.04	0.03	1.18	1.94

Table 4.10 gives the magnitudes of individual harmonics at the single phase inverter output in amperes. It emphasizes that the increment in I_{THD}% merely caused by the reduction in output current of the inverter even if the low order harmonics like 3rd and 5th order harmonics are lowered.

Table 4.10: Individual current harmonic magnitudes at S1 inverter output

Harmonic Order (h)	Single Phase Inverter (S1)	
	Magnitude in Ampere	
	1000 Wm^{-2}	500 Wm^{-2}
1	8.78	4.79
3	0.13	0.08
5	0.03	0.01
123	0.03	0.03
125	0.08	0.08
127	0.02	0.02

5. PROPAGATION OF NETWORK HARMONICS

In this chapter, harmonic injection into the distribution network from a solar PV system is simulated as a harmonic injector which is a combination of sinusoidal current source and harmonic generation unit. Harmonic propagation is examined with different contribution levels as percentages of feeder loading. In view of the working of a solar PV system, it is a power converter which can generate a sinusoidal current with harmonics. A solar PV inverter can be modeled as a current source which produces a sinusoidal current output with a controllable magnitude and phase angle. This sinusoidal current is synthesized by controlling the real and reactive components of the output current.

5.1. Current Source Inverter (Harmonic Injector)

Figure 5.1 (a) shows a simplified equivalent circuit of the Current Source Inverter (CSI) which produces output current (I_{pv}) and the output synchronized voltage (V_{pv}).

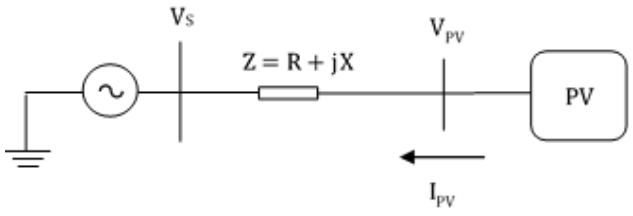

(a)

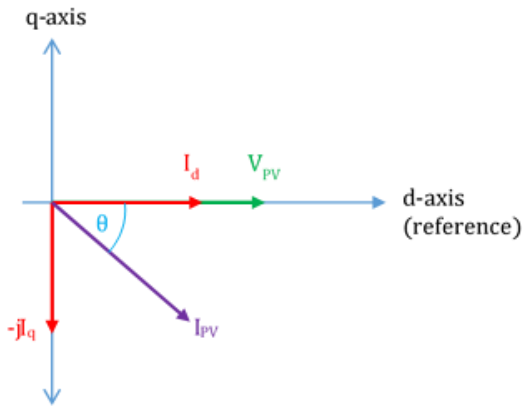

(b)

Figure 5.1: (a)- Simplified equivalent circuit of PV integration (b)- I_{pv} in d-q frame

They can be represented in a complex plane (the synchronous d-q frame) such that the real current component Id as d-axis component and the reactive current component Iq as q-axis component as shown in Figure 5.1 (b). These Id and Iq can be used to control the real and reactive power output of the inverter [10][41].

The complex form of the output quantities of the inverter is given by Eqn. (5.1) and (5.2).

$$V_{out} = V_{PV}e^{j0} \tag{5.1}$$

$$I_{out} = I_{PV}e^{-j\theta} \tag{5.2}$$

The complex power S_{out} is defined as

$$S_{out} = VI^{*} = V_{PV}e^{j0} \cdot I_{PV}e^{j\theta} = V_{PV}I_{PV}e^{j\theta} = Se^{j\theta} \tag{5.3}$$

The magnitude of the complex power is called the apparent power and can be expressed in Volt-Amperes as

$$S = VI \tag{5.4}$$

The real power is

$$P = \mathrm{Re}[S_{out}] = V_{PV}I_{PV}\cos\theta \tag{5.5}$$

The reactive power is

$$Q = \mathrm{Im}[S_{out}] = V_{PV}I_{PV}\sin\theta \tag{5.6}$$

PSCAD library model of current source is used with an external current input which is controlled at the desired magnitude and phase. Synchronizing occurs at the control loop of the CSI. With reference to Figure 5.2, the input signal to the current source (I_{out}) is a combination of the regulated fundamental current signal and desired signals at different frequencies (integer multiples of fundamental frequency) to represent harmonics.

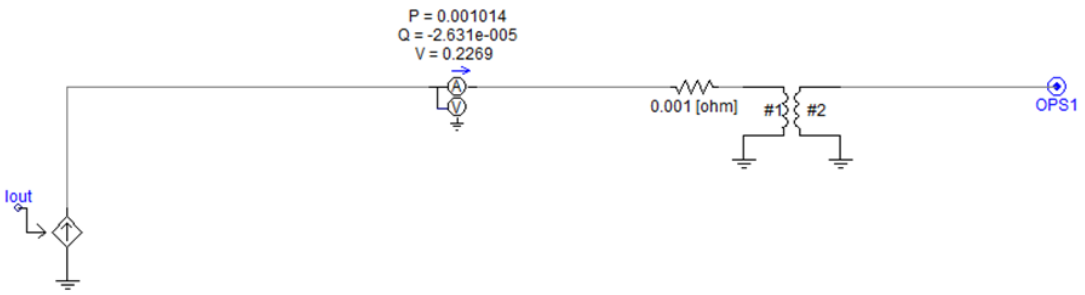

Figure 5.2: Grid Integration of CSI

Magnitudes of these harmonic components were considered as a percentage of the rated current to comply with the standard constraints IEC 61800-3[9].

Figure 5.3 shows the control functions of real and reactive power to operate the CSI at unity power factor. It is controlled with the reference frame at the POC of the inverter. Therefore, the reference is the voltage at the POC of the inverter (VS1). V_{pv}, P_{pv} and Q_{pv} are measured quantities at the output terminal of the inverter.

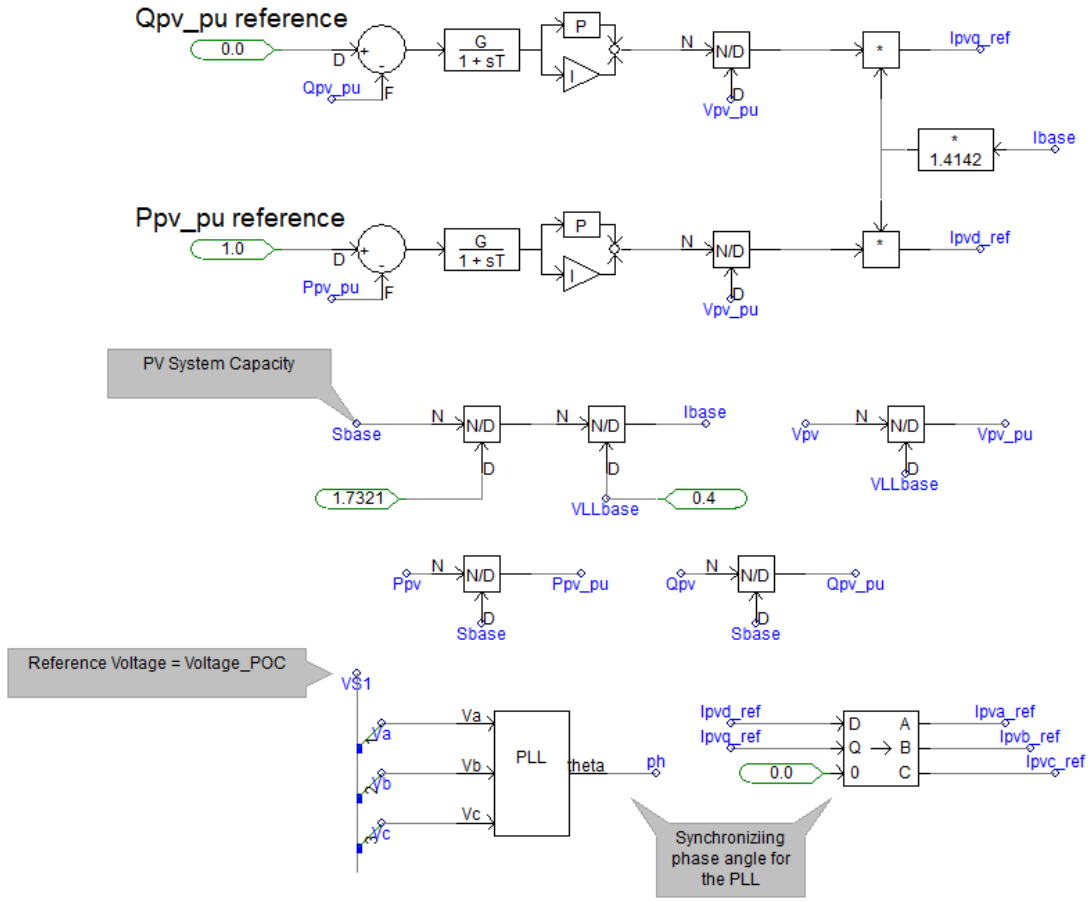

Figure 5.3: Control functions of CSI

Three phase current source inverter contains three number of PSCAD current sources to generate three phases with the phase difference of 120^0 in between them.

5.2. Harmonic generation Unit

Sinusoidal waveform generator can be used simply to produce harmonic components at required frequencies, providing the phase, frequency and magnitude. Then, they are

combined using summing junction to form the distorted signal. An example of a distorted waveform is presented in Figure 5.4. In signal summation unit, for the harmonic injector the fundamental current signal is replaced with the reference signal generated by the control functions (refer Figure 5.3).

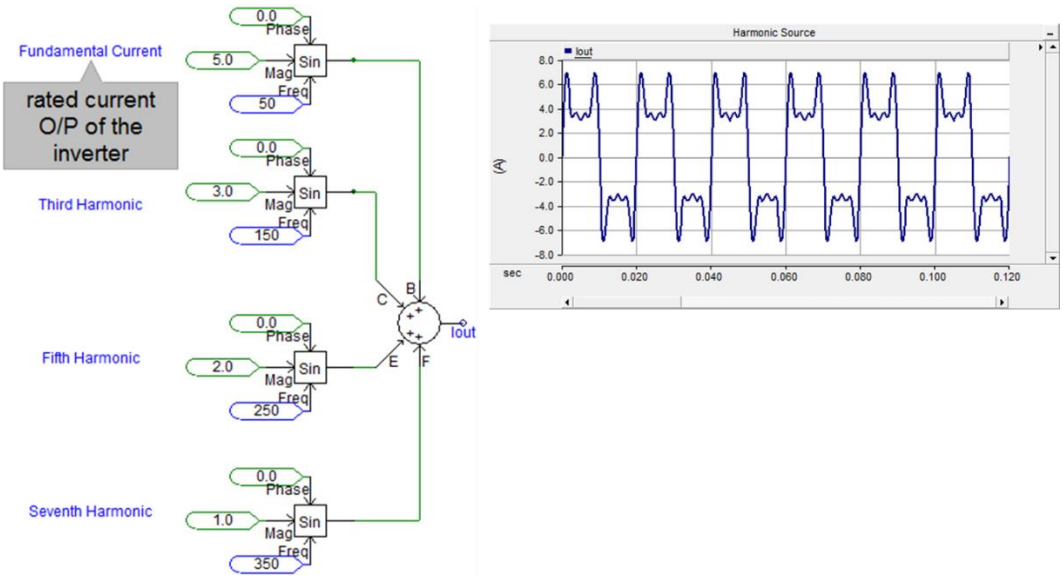

Figure 5.4: Summation of 3rd, 5th and 7th harmonics to the fundamental signal

Harmonic generator can produce the distorted current signal at desired value. Some examples are given as follows.

Example 1: 3rd, 5th and 7th harmonics were added to the fundamental current of 5 kA. The details are provided in Table 5.1. Figure 5.5 shows the amount of distortion of the signal.

Table 5.1: Individual harmonic magnitudes

Harmonic Order	Magnitude (kA)
3	0.192
5	0.126
7	0.097

$$THD\ \% = \frac{\sqrt{0.192^2 + 0.126^2 + 0.097^2}}{5} \times 100$$

$$= 0.0498\ \times 100$$

$$\cong 5\ \%$$

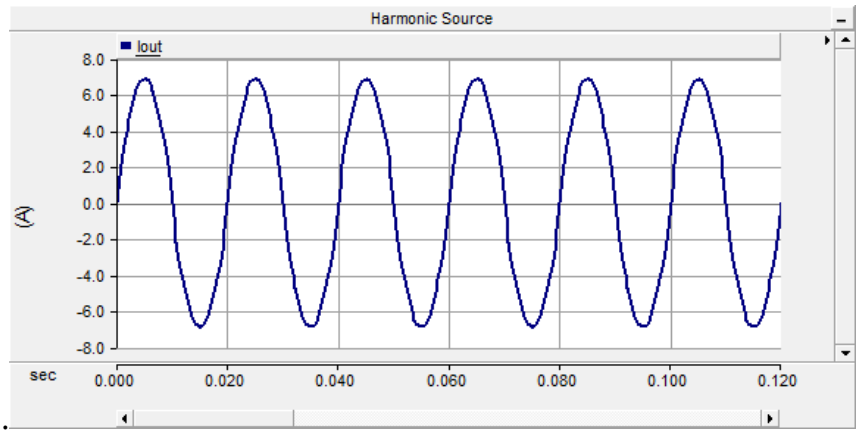

Figure 5.5: Current waveform distortion at 5% of I_{THD}

Example 2: 5^{th}, 7^{th} and 9^{th} were added to the fundamental current of 5 kA. The details are provided in Table 5.2. Figure 5.6 shows the amount of distortion of the signal.

Table 5.2: Individual harmonic magnitudes

Harmonic Order	Magnitude (kA)
5	0.281
7	0.345
9	0.413

$$THD\ \% = \frac{\sqrt{0.281^2 + 0.345^2 + 0.413^2}}{5} \times 100$$

$$= 0.1214\ \times 100$$

$$\cong 12\ \%$$

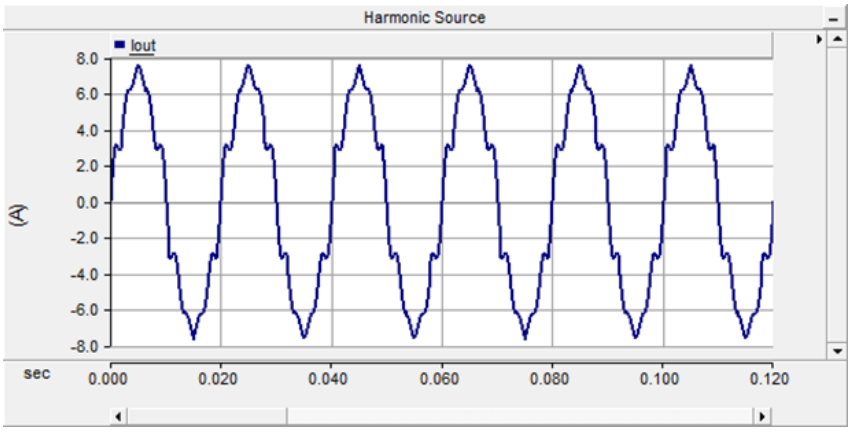

Figure 5.6: Current waveform distortion at 12 % of I_{THD}

5.3. Results of simulation for harmonic penetration

Similarly, six number of PV integrations were done including three single phase inverters and three three phase inverters at same POC s. In addition to the six number of locations numbered from 1 to 6, location 0 where the primary side of the distribution transformer was chosen to examine the harmonic propagation. Harmonic measuring locations and the POCs of inverters are as shown in Figure 5.7.

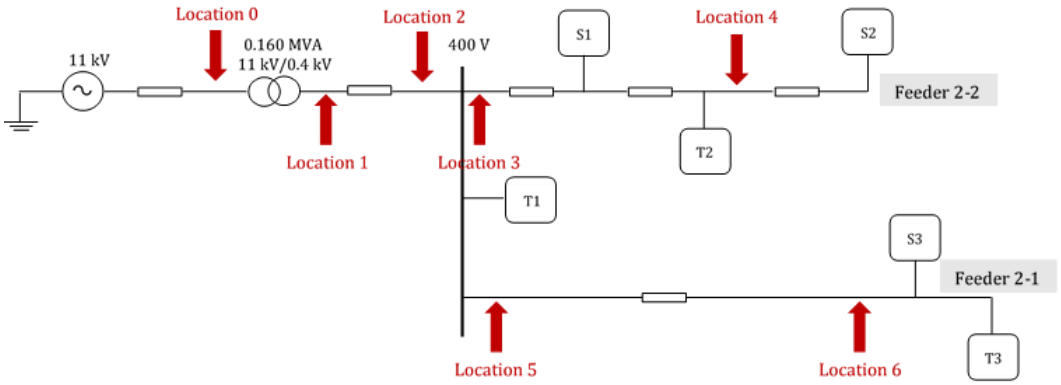

Figure 5.7: Schematic of PV (harmonic injector) integrations

The analysis was conducted in four different case studies. Three of them were carried out by changing the PV penetration as percentage of feeder loading. Considering high PV penetration, 50%, 70% and 90% of feeder loading were fed by PV systems.

According to the limitations discussed in [1], low order odd harmonics were injected as expressed in (5.7) and (5.8)

$$h < 11 \quad (5.7)$$

$$I_h \leq 0.04\ I_{rated} \quad (5.8)$$

Where, h = harmonic order

I_h = harmonic current magnitude in Ampere

Case 1 – PV penetration with 50% of feeder loading

To obtain 50% of active power, PV systems were operated under the conditions tabulated in Table 5.3.

Table 5.3: PV system operation conditions in Case 1

Inverter Type	No. of CSIs	Capacity (kW)	Rated rms Current (A)	Injected Harmonic magnitudes (A)		
				h = 3	h = 5	h = 7
Single Phase	3	1	4.34	0.17	-	-
Three Phase	2	5	7.21	-	0.29	-
Three Phase	1	7	10.10	-	0.40	-

PV integrations illustrated in Figure 5.8 with harmonic magnitudes.

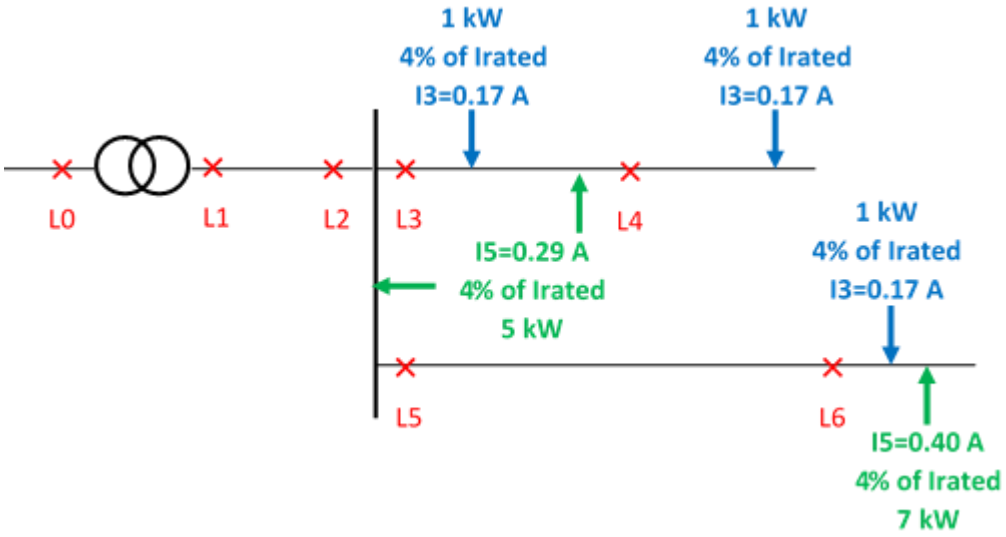

Figure 5.8: Harmonic injection of inverters in Case 1

V_{THD}% and I_{THD}% were measured at seven locations numbered from 0 to 6. The results are shown in Table 5.4.

The power flow is in the usual direction with PV integrations. The currents flowing in these locations are different from the values of no PV integrations. Individual harmonics are in phase with their corresponding order.

At Location 1,

$I_3 = 0.49$ A

Table 5.4: THD% at seven different locations in Case 1

rms Current Magnitudes	L0	L1	L2	L3	L4	L5	L6
Fund (A)	1.65	37.85	30.39	9.57	4.23	19.29	10.81
h=3 (A)	0.01	0.49	0.49	0.33	0.17	0.16	0.17
h=5 (A)	1×10^{-4}	0.95	0.96	0.28	0.005	0.39	0.40
h=7 (A)	7×10^{-5}	0.002	0.001	7×10^{-4}	2×10^{-4}	0.001	1×10^{-4}
I_{THD}%	0.64	2.85	3.55	4.59	3.98	2.18	4.02
V_{THD}%	0.01	0.08	0.09	0.09	0.10	0.09	0.11

It is approximately equal to the arithmetic summation of all three 3rd order harmonics injected by single phase CSI s as in Eqn. 5.9.

$$I_3 \simeq 0.17 \times 3 = 0.51 \text{ A} \tag{5.9}$$

At Location 0,

$I_3 = 0.01$ A

It is approximately equal to the transformed value of I_3 at Location 1 where the secondary side of the transformer as in Eqn. 5.10. It implies that triplen harmonics can be observed in the upstream of the distribution transformer due to the unbalanced single phase PV integrations.

$$I_3 \approx \frac{0.49\times0.4}{11} = 0.018 \text{ A} \tag{5.10}$$

At Location 0,

$I_5 = 3 \times 10^{-4}$ A

The magnitude of the 5th order harmonic is lower than the transformed value as in (5.11).This attenuation occurs when the harmonic current passing through the distribution transformer as it behaves as a high impedance inductor.

$$I_5 < \frac{0.95\times0.4}{11} = 0.034 \text{ A} \tag{5.11}$$

Though 7th order harmonic is not injected, its magnitude is measured to check for any interactions among different harmonic orders. Results show that there is no any interaction among 3rd, 5th and 7th order harmonics as the values are negligible.

Case 2 – PV penetration with 70% of feeder loading

Six number of PV systems were operated as given in Table 5.5 to inject 70% of active power of the feeder loading.

Contribution of three phase CSI s is increased to produce required active power, aiming to reduce the unbalance in PV integration. PV integrations are illustrated in Figure 5.9 with the magnitudes of injected harmonics. The measured values at seven locations are presented in Table 5.6.

Table 5.5: PV system operating conditions Case 2

Inverter Type	No. of CSI s	Capacity (kW)	Rated rms Current (A)	Injected Harmonic magnitudes (A)		
				h = 3	h = 5	h = 7
Single Phase	3	1	4.34	0.17	-	-
Three Phase	2	8	11.54	-	0.46	-
Three Phase	1	9	12.99	-	0.52	-

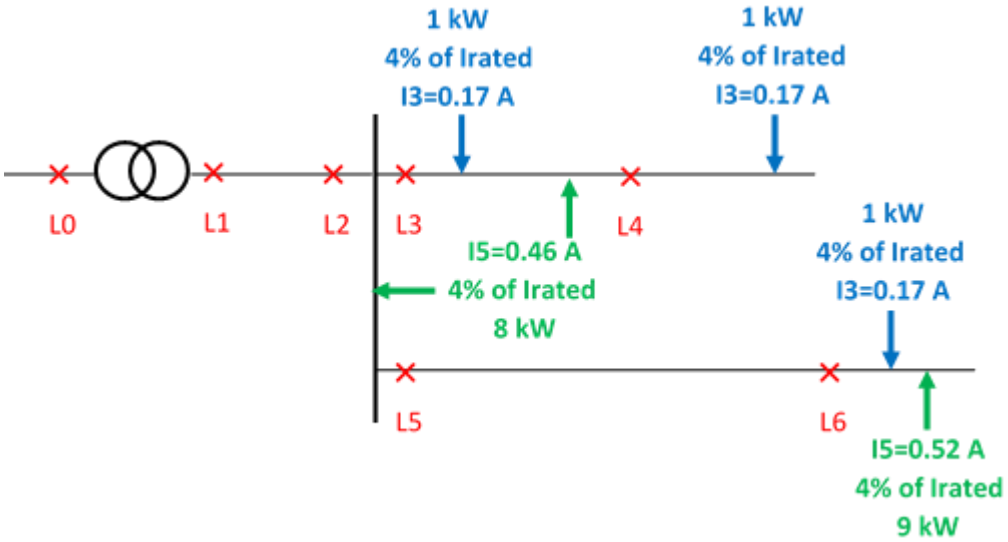

Figure 5.9: Harmonic injection of inverters in Case 2

Table 5.6: THD% at seven different locations in Case 2

rms Current Magnitudes	L0	L1	L2	L3	L4	L5	L6
Fund (A)	1.55	36.23	30.95	11.07	4.21	18.54	13.83
h=3 (A)	0.01	0.49	0.49	0.33	0.17	0.16	0.17
h=5 (A)	1×10^{-4}	1.39	1.40	0.45	0.008	0.49	0.51
h=7 (A)	7×10^{-5}	0.002	0.001	5×10^{-4}	2×10^{-4}	0.001	1×10^{-4}
I_{THD}%	0.68	4.09	4.80	5.07	3.99	2.81	3.90
V_{THD}%	0.01	0.11	0.13	0.13	0.14	0.13	0.17

The power flow has been changed in two locations with PV integrations as more active power is injected to the grid. In Location 3 and Location 6, current flows towards the 400 V bus. It shows that harmonic current flow does not depend on the direction of the fundamental current. The flow of harmonic currents is towards the distribution transformer (delta-wye) to complete its path. They arithmetically add up towards the distribution transformer as they are in phase in this case study.

At Location 1,

$I_5 = 1.39$ A

5th order harmonic is approximately equal to the summation of all injected 5th order harmonic magnitudes as in (5.12).

$$I5 \approx (0.46 \times 2) + 0.52 = 1.44 \text{ A} \quad (5.12)$$

Case 3 – PV penetration with 90% of feeder loading

To improve the active power penetration, capacity of three phase CSI s were increased. Six PV systems performed as given in Table 5.7. Simulation results are given in Table 5.8. PV integrations are illustrated in Figure 5.10.

Results confirm that I_{THD}% at particular location in one feeder (branch) is affected by the current harmonics injected to the same feeder (branch) only.

At Location 5 and 6,

$I_3 = 0.16$ A, $I_5 = 0.55$ A and $I_3 = 0.17$ A, $I_5 = 0.57$ A

Table 5.7: PV system operating conditions Case 3

Inverter Type	No. of CSI s	Capacity (kW)	Rated rms Current (A)	Injected Harmonic magnitudes (A)		
				h = 3	h = 5	h = 7
Single Phase	3	1	4.34	0.17	-	-
Three Phase	2	10	14.43	-	0.58	-
Three Phase	1	13	18.76	-	0.75	-

I_3 and I_5 magnitudes are equal to the current harmonic magnitudes; I_3 injected by the single phase CSI (S3) and I_5 injected by the three phase CSI (T3).

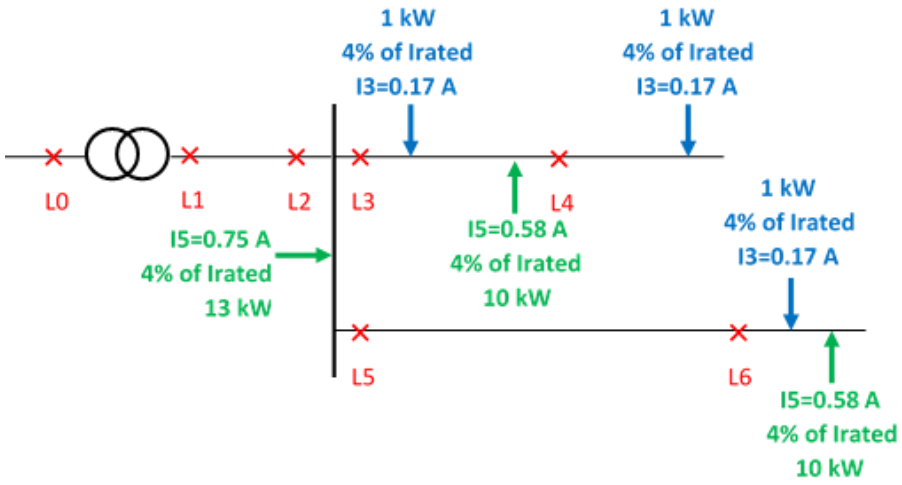

Figure 5.10: Harmonic injection of inverters in Case 3

. Table 5.8: THD% at seven different locations in Case 3

rms Current Magnitudes	L0	L1	L2	L3	L4	L5	L6
Fund (A)	1.42	34.42	31.99	12.11	4.19	17.21	15.16
h=3 (A)	0.01	0.49	0.49	0.33	0.17	0.16	0.17
h=5 (A)	9×10^{-5}	1.85	1.85	0.56	0.01	0.55	0.57
h=7 (A)	7×10^{-5}	0.002	0.001	5×10^{-4}	2×10^{-4}	0.001	1×10^{-4}
I_{THD}%	0.74	5.56	5.99	5.39	4.02	3.32	3.91
V_{THD}%	0.01	0.15	0.17	0.17	0.18	0.17	0.21

Case 4 – All inverters are at the limit of I_{THD}%

Low order harmonics; 3rd, 5th, 7th from single phase inverters and 5th, 7th from three phase inverters were injected to the grid at same POC s. Magnitudes were determined to have the maximum permissible I_{THD}% at POC s. for this case, 70% of feeder loading was provided by the PV installations. PV systems were operated as in Table 5.9.

Table 5.9: PV system operating conditions in Case 4

Inverter Type	No. of CSI s	Capacity (kW)	Rated rms Current (A)	Injected Harmonic magnitudes (A)		
				h = 3	h = 5	h = 7
Single Phase	3	1	4.34	0.17	0.08	0.08
Three Phase	2	8	11.54	-	0.46	0.34
Three Phase	1	9	12.99	-	0.52	0.39

PV integrations with operating conditions are illustrated as in Figure 5.11.

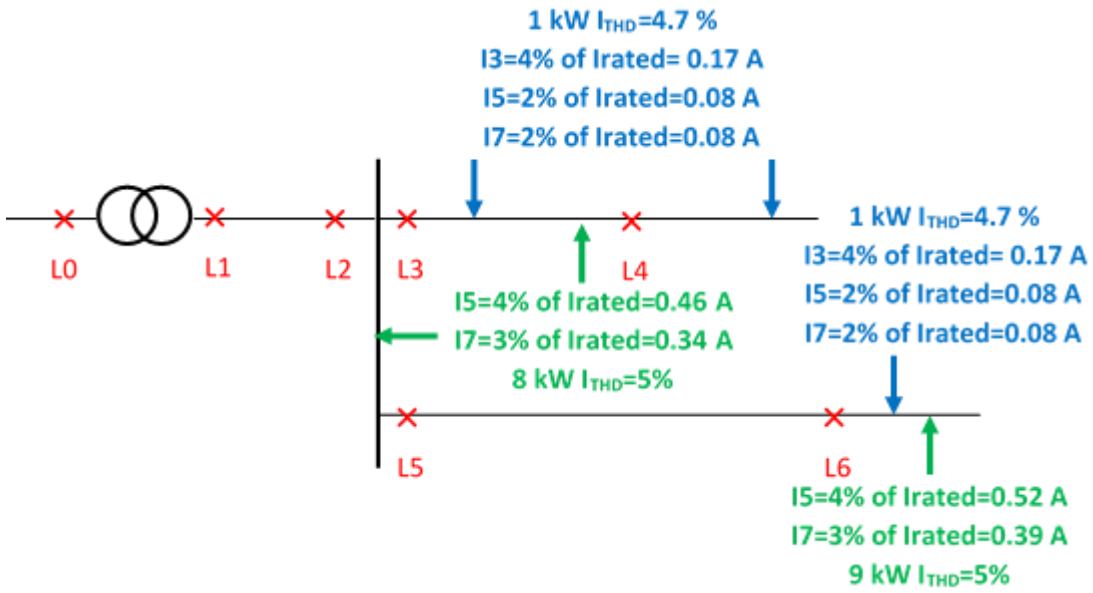

Figure 5.11: Harmonic injection of inverters in Case 4

Low order harmonics 3rd, 5th and 7th were measured at seven locations and tabulated in Table 5.10. Magnitudes are rms harmonic currents in Ampere.

The similar observations were recorded as in previous cases. It confirmed that the harmonic currents in phase are added up towards the distribution transformer for the same frequency.

At Location 0,

$I_3 = 0.01 \approx (0.49 \times 0.4)/11 = 0.018$ (5.13)

Table 5.10: THD% at seven different locations in Case 4

rms Current Magnitudes	L0	L1	L2	L3	L4	L5	L6
Fund (A)	1.47	33.96	28.66	10.49	4.21	17.79	13.70
h=3 (A)	0.01	0.49	0.50	0.33	0.17	0.16	0.17
h=5 (A)	0.003	1.55	1.55	0.60	0.07	0.57	0.59
h=7 (A)	0.003	1.19	1.19	0.48	0.07	0.44	0.46
I_{THD}%	0.78	5.94	7.05	8.05	4.71	4.17	5.61
V_{THD}%	0.01	0.19	0.22	0.22	0.24	0.24	0.29

As given in (5.13), I_3 is approximately equal to the transformed value from secondary side of the distribution transformer to the primary side. But, I_5 and I_7 are attenuated when they travel to the upstream through the distribution transformer as shown in (5.14) and (5.15).

$$I_5 = 0.003 < \frac{1.55 \times 0.4}{11} = 0.056 \quad (5.14)$$

$$I_7 = 0.003 < \frac{1.19 \times 0.4}{11} = 0.043 \quad (5.15)$$

Chapter 6

6. DISCUSSION AND CONCLUSION

6.1. Discussion

Motivation of using solar PV technology due to the preferential allowances granted by the Sri Lankan government increases the number of grid connected small scale PV systems which causes technical, operational and control problems in LV power grid. Mainly for power quality issues such as voltage unbalance, local voltage rise, voltage fluctuations, the mitigation techniques have been discussed in the literature. Based on past research studies further analysis of harmonic penetration and harmonic propagation in the distribution network is essential to improve existing regulations of grid connected PV systems in Sri Lanka

In this research study, harmonic generation from a PV system, effect of multi-inverter operation on harmonics, effect of solar irradiance on harmonics, effect of POC of the inverter on harmonics and the harmonic propagation in the distribution feeder are discussed with a detailed simulation model of a PV system. In order to execute the analysis of harmonic propagation in the distribution network, a harmonic injector was modeled which behaves as a PV system.

The detailed model of the PV system was built up with typical components of PV array, DC-DC (buck) converter, Inverter Bridge and LCL filter. PSCAD library model of solar PV array was fed with STC values of 1000 W/m^2 and 25^0C. Therefore no dynamic behavior can be observed and examined. But, the input quantities of the solar PV array; solar irradiance and temperature can be varied in the design. To investigate the effect of solar irradiance on harmonic magnitudes, it was reduced to achieve the 50% of shading. Even though the MPPT ensures the MPP voltage, the output of the PV array is reduced. Accordingly it lowers the output current of the PV system which leads to a higher total harmonic distortion of current. In a situation which that the I_{THD}% exceeds the standard limits total demand distortion has been defined to quantify the harmonic distortion. In this study, I_{THD}% s do not violate the standard limitations given in IEC61000-3-2:12.

Although the dynamic behavior is not considered, in order to examine the harmonic generation of a PV system accurately and to accomplish the actual behavior of a PV system, MPPT has been used in this research work as well. More accurate and less complex Incremental Conductance algorithm is selected in PSCAD MPPT unit. DC-DC converter is used to provide appropriate dc voltage for the inverter bridge by stepping up or stepping down the output voltage of the PV array. This can be eliminated with proper selection of the PV array to match its output voltage for the inverter at desired value. Most probably, in small scale PV installations a DC - DC converter should be deployed. In this model DC - DC buck converter was used to step down the output voltage (MPP Voltage) of the PV array in both single phase and three phase PV systems.

DC - AC inverter is formed with IGBT power electronic switches; H-bridge (two pair of legs) and inverter bridge with three pair of legs are respectively for single phase and three phase inverters. Most commonly used switching techniques are bi-polar SPWM and uni-polar SPWM. From these two techniques, bipolar SPWM is used in these simulation models to generate the AC output. Frequency modulation index was selected to be an odd integer to restrict the presence of even harmonics and inter-harmonics in the output harmonic spectrum. Amplitude modulation index was chosen to achieve the linear modulation which gives minimum low order harmonics at the inverter output. In bi-polar modulation, reference voltage signal (the voltage at the POC) is compared with the triangular signal to produce switching signals for the IGBT switches in the inverter bridge. In the literature, there are some switching techniques developed and proven to present minimum harmonic levels at the inverter output. But SPWM is simple and efficient even though it is conventional.

The output of the inverter is connected to the grid through a LCL filter. LCL filter is recommended by most of the researchers with a list of advantages over other passive filters. The filter parameters; inverter side inductance, grid side inductance, filter capacitance and damping resistance were determined following a most popularly used a set of equations which has been proven for its better performances in the literature. Single phase and three phase inverters were performed well. Their THD% values of voltage and current are within the standard harmonic limits in IEC61000-3-2:12.

This PV system model is connected to the grid without an isolation transformer. Adding an isolation transformer increases losses, cost and weight of a PV system. Therefore, isolation transformers are not added up to the domestic roof top (small scale) PV systems. But it can be used as a harmonic mitigation technique.

At present, higher number of solar PV integrations is reported in kotte area. Therefore, one of the feeder from Pitakotte area was selected. actual feeder loading data of that particular feeder were used to model the distribution feeder. Upstream utility grid was modeled as an equivalent voltage source with a series impedance. The series impedance ($R+j\omega L$) was determined to represent a weak network, considering fault levels at several PSS s and making an assumption of the distance to the distribution transformer from a PSS. The aim was to examine the impact of harmonics in a weak network. Because harmonic distortion is to be worsen in a weak network. In comparison of strong, intermediate and weak network characteristics, the impact via the distribution transformer to the downstream is not noticeable.

To investigate the harmonic propagation in the distribution feeder, a harmonic injector was designed in which the harmonic magnitudes can be changed as desired. Grid synchronization is accomplished with park transformation and phase locked loop unit for detecting the synchronizing phase angle. This mechanism is the best and frequently used grid synchronization mechanism in published literature which provides a good controlling of active and reactive power of a PV system. This current source inverter (harmonic injector) is strictly operated at unity power factor. Low order harmonic magnitudes of 3^{rd}, 5th and 7^{th} were changed as a percentage value of the nominal current of a particular inverter capacity.

6.2. Conclusions

Research work presented in this thesis based on the simulation results of PV system integrations in a LV distribution network.

The detailed model of a PV system discussed in chapter 3 is very useful to identify and understand the behavior of a PV system. As the input quantities of the PV array; the solar irradiance and the temperature were designed in a way that can be varied, it can be used to evaluate the effect of variation of solar irradiance and

temperature. The conclusions made with results of detailed model integrations can be listed as follows;

- Linear modulation minimizes the low order harmonics. High order harmonics which are at the switching frequency and its side bands are appeared in the harmonic spectrum of voltage and current. Asynchronous PWM is avoided by selecting the switching frequency to make the frequency modulation index an odd integer. Further, even harmonics are not appeared at the inverter output. Results confirms that the harmonic production of three phase inverter is less than the single phase inverter.
- In multiple operation of PV systems, current THD is being reduced while voltage THD is being increased. The reduction in current THD is caused due to the attenuation in individual current harmonics. The boost in voltage THD is caused by the increase in background voltage distortion level due to multi-inverter integrations.
- When the POC of a particular inverter is apart from the distribution transformer, the influence of the increment of grid impedance results in a growth in voltage THD at the inverter output.
- Decrease in solar irradiance reduces the power output of the PV array. Therefore, output current is lowered. Then it causes higher current THD at the inverter output.
- THD values of current in the locations of the distribution feeder are highly influenced by the fundamental current flowing in the respective location. Multiple PV integrations differ the normal power flow due to the active power penetration of PV systems. In some locations, current THD reaches very high percentage values.

Harmonic injector design developed in chapter 5 is a supportable unit to investigate the harmonic injection and propagation in the distribution network by varying the capacity and the magnitudes of harmonics as desired. Simulation results of harmonic propagation obtained with harmonic injector can be summarized as follows;

- Individual harmonics travel towards the distribution transformer during the fundamental current does the power distribution to the loads.
- Individual harmonics at the same frequency arithmetically add up in the direction of harmonic current flow.
- As the frequency is increased, individual harmonics do not propagate to the upstream via the distribution transformer as the transformer behaves as a high impedance reactor and restricts transferring them to the primary side of the transformer.
- As a result of uneven distribution of single phase PV system integrations, triplen harmonics are appeared in the distribution network and low order triplen harmonics are propagated to the primary side of the distribution transformer.

LIST OF REFERENCES

[1] B. Robinson, "Energy Resources Types", GEOE432:Energy Policy, John A. Dutton e-education Institute, college of Earth and Minaral Sciences, Univ. Pennsylvia State [online], http://www.e-education.psu.edu/geog432/.

[2] P. Komor and T. Molnar, "Background Paper on Distributed Renewable Energy Generation and Integration" University of Colorado, Boulder, Colorado, USA, 20 February 2015.

[3] The Gazette of the Democratic Socialist Republic of Sri Lanka-extraordinary, Part I: Section (I)-General,No. 1553/10 – Tuesday, June 10, 2008.

[4] Sri Lanka Energy Sector Development Plan For A Knowledge- Based Economy 2015 – 2025, Ministtry of Power and Energy

[5] Sri Lanka Energy Balance [online], available at: http://www.energy.gov.lk

[6] D.G. Infield et al, "Power quality from multiple grid-connected single phase inverters," IEEE Trans. On Power delivery, Vol.19 (4), pp.1983-1989, Oct 2004.

[7] D. Perera, "Contributions to the understanding of harmonics, flicker and voltage unbalance managements in future electricity distribution network," Ph.D dissertation, School of Electrical, Computer and Telecommunications Eng., Univ. Wollongong, New South Wales, Australia, 2014.

[8] A. Chidurala et al, "Harmonic Characterization of Grid Connected PV Systems & Validation with Field Measurements", ©2015 IEEE.

[9] Grid Connection Requirement for Solar Power Plants – Addendum to the CEB Guide for Grid Interconnection of Embedded Generators, December 2000.

[10] N. Mohan, " Review of Basic Electrical and Magnetic Circuit Concepts," in Power Electronics Converters, Applications and Design, 2nd ed., New York, John Willey and Sons, Inc., 1995, ch.3, pp. 33 - 60.

[11] J. R. Lucas, "Theory of Electricity – Analysis of Non-sinusoidal Waveforms - Part 1," Dept. Elec. Eng., Univ. Moratuwa, Oct 2001.

[12] IEEE Interharmonic Task Force, Cigré 36.05/CIRED 2 CC02 Voltage Quality Working Group, "Interharmonics in Power Systems,"

[13] R. C. Dugan *et al*, "fundamentals of Harmonics", in Electrical Power system quality, 2nd ed., New York McGrow-Hill, ch.5, pp. 167 – 224, www.digitalengineering library.com.

[14] J. Smith *et al*, "Power Quality Aspects for Solar Power," working Group JWG C4/C6.29, Dec 2016.

[15] N. Mohan, "Switch-mode dc-ac Inverters: dc Sinusoidal ac," in Power Electronics Converters, Applications and Design, 2nd ed., New York, John Willey and Sons, Inc., 1995, ch. 8, pp. 200 – 215.

[16] A. Y. Kalbat, "PSCAD simulation of grid-tied photovoltaic systems and total harmonic distortion analysis, IEEE Conference Publication, pp. 1-6, 2013.

[17] D.G. Infield *et al*, "Power quality from multiple grid-connected single phase inverters," *IEEE Trans. On Power delivery,* Vol.19 (4), pp.1983-1989, Oct 2004.

[18] J.H.R. Enslin *et al*, "Harmonic interaction between a large number of distributed power inverters and the distribution network," *IEEE Trans. On Power electronics,* Vol. 19(6), pp.1586-1593, Nov 2004.

[19] A. Chidurala et al, "Harmonic impact of high penetration photovoltaic system on unbalanced distribution networks – learning from an urban photovoltaic network," IET Renewble Power Generation, Vol. 6 (4), pp 485-494, 2016.

[20] A. Celebi and M. Cloak, "The effects of harmonic produced by grid connected photovoltaic systems on electrical networks," Dept. Elec. & Electronic Eng., Fac. Eng., Ege Univ., Bornova.

[21] E.C. Aprilia, "Modelling of Photovoltaic (PV) Inverter for Power Quality Studies," MSc. Dissertation, Dept. Electrical Eng., Univ. Eindhoven, North Brabant, Netherlands, 2012.

[22] H. Hu et al., "Potential Harmonic Resonance Impacts of PV Inverter Filters on Distribution Systems," IEEE Trans. On Sustainable Energy, vol. 6(1), Jan 2015.

[23] M.S. de Cardona and J. Carretero, "Analysis of the current total harmonic distortion for different single-phase inverters for grid-connected pv-systems," Applied Physics Dept. II, Univ. Malaga, Malaga, Spian, 2004.

[24] M. Patsalides et al, "The effect of solar irradiance on the power quality behaviour of grid connected photovoltaic systems," Dept. Elec. And Comp. Eng., Univ. Cyprus.

[25] G. K. Venayagamurthy, "Comparison of Power System Simulations Studies on Different Platforms – RSCAD, PSCAD/EMTDC and SIMULINK SimPowerSystems," Real-time Power and Intelligent Systems Laboratory, Univ. Missouri-Rolla, USA.

[26] A. D. Rajapakse and D. Muthumuni, "simulation Tools for Photovoltaic System Grid Integration Studies," IEEE Conf. Electrical Power and Energy, 2009.

[27] A. Kalbat, "PSCAD Simulation of Grid-Tied Photovoltaic Systems and Total Harmonic Distortion Analysis," 3rd Int. Conf. on Electric Power and Energy Conversion Systems, Turkey, ©2013IEEE.

[28] M. H. Tushar, "Comparative Study on DC-DC Converters," Dept. Elec & Elect. Eng, Univ. BRAC, Dhaka, Bangladesh, 2012.

[29] MICROCHIP Webseminar, "Buck Converter Design Example," Microchip Technology Inc, 2006.

[30] N. Mohan, "Overview of Power Electronic Semiconductor Switches," in Power Electronics Converters, Applications and Design, 2nd ed., New York, John Willey and Sons, Inc., 1995, ch.2, pp. 16 - 32.

[31] J. Lettl et al., "Comparison of Different Filter Types for Grid Connected Inverter," Progress in Electromagnetics Research Symposium Proc., pp.1426 -1429, March 2011.

[32] T. C.Y. Wang et al., "Output Filter Design for a Grid-interconnected Three-phase Inverter," GE Global Research Center, New York, pp.779 –784, ©2003 IEEE.

[33] A. Reznik et al., "LCL Filter Design and Performance Analysis for Grid Interconnected Systems," IEEE Trans. on Industry Applications, Vol. 50 (2), March/April 2014.

[34] Public Utilities Commission of Sri Lanka, "Generation and Reservoirs Statistics-March 20, 2018," [online], available at: http://www.pucsl.gov.lk/english/wp-content/uploads/2018/03/Generation-Report_20-03-2018.pdf

[35] Ceylon Electricity Board, "Historical Data Book 1969-2015" [online], available at: http://www.ceb.lk/index.php?aam_media=38068

[36] L. N. W. Arachchige *et al.*, "Generation cost Optimization through a Network Stability study," Dept. Elec. Eng., Univ. Moratuwa, July 2016.

[37] Lanka Electricity Company (Private) Limited, “Load Flow Analysis – Year 2015 to 2025,” Dept. System Development, April 2015.

[38] D.H.O. McQueen *et al.*, “Monte Carlo Simulation of Residential Electricity Demand for Forecasting Maximum Demand on Distribution Networks,” IEEE Trans. On Power Systems, Vol.19 (3), pp.1685-1689, Aug 2004.

[39] M. Sun et al., “Analysis of Diversified Residential Demand in London Using Smart Meter and Demographic Data,” Power and Energy Society General Meeting (PESGM), July 2016©IEEE.

[40] P. Kundur, “Power System Loads,” in Power System Stability and Control, NewYork, McGraw-Hill, Inc., ch. 7, pp. 271 – 313.

[41] E. Muljadi et al., “ User Guide for PV Dynamic Model Simulation Written on PSCAD Platform,” Technical Report, National Renewable Energy Laboratory, U.S. Dept. of Energy, Nov 2014 – www.nrel.gov/publications

APPENDIX A – DRAWING OF PITAKOTTE DISTRIBUTION AREA

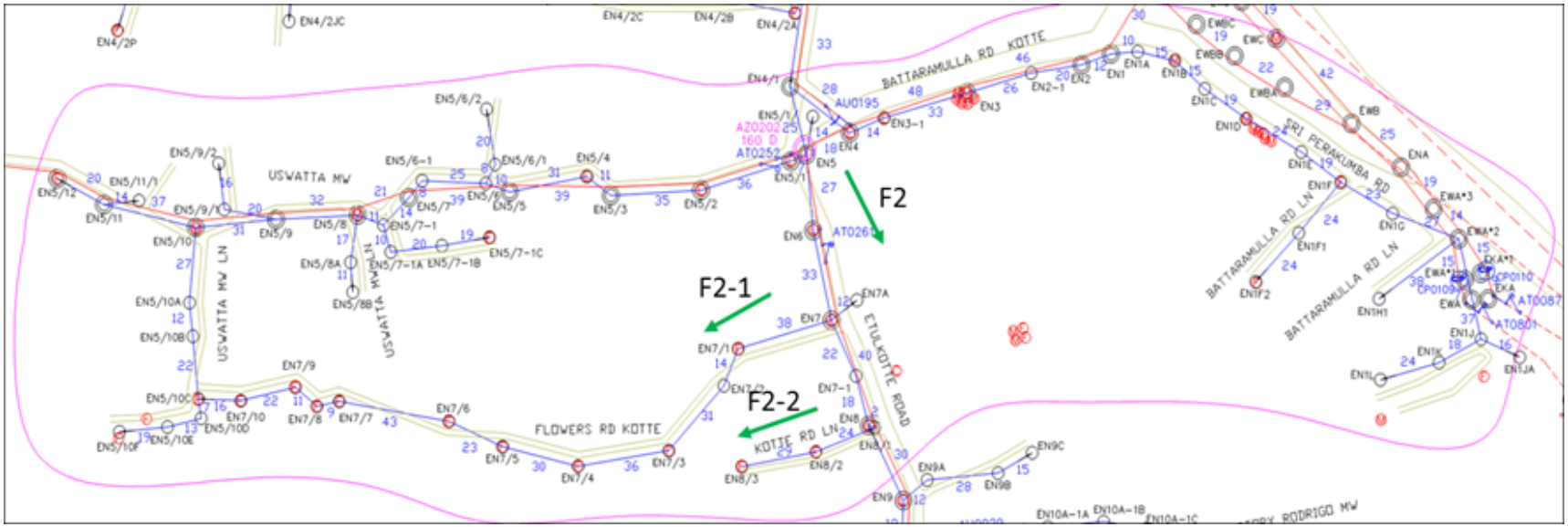

APPENDIX B – PSCAD MODEL OF THE COMPLETE SYSTEM WITH PV INTEGRATIONS